



Clean Air Partners

5066 Santa Fe Street, San Diego, CA 92109
Phone: (858) 581-5600 Fax: (858) 581-5626

Report: 010043
Date: October 11, 2001

Laboratory Development of the Enhanced Caterpillar C12 Dual-Fuel Truck Engine

Subcontract No. ACI-9-18055-01

(Between BKM and NREL)

and

Contract No. 99157

(Between CAP and AQMD)

Final Report

Submitted to:

Mr. Mike Frailey of National Renewable Energy Laboratory

and

Mr. Mike Bogdanoff of South Coast Air Quality Management District

by:

H. C. Wong

Program Manager & Principal Investigator

hcwong@bkm-inc.com

EXECUTIVE SUMMARY

This report details work conducted under BKM Project 25740, "On-Road Development of Enhanced Caterpillar® C-12 Dual-Fuel™ Truck Engine." This project was sponsored by:

1. The National Renewable Energy Laboratory (NREL) under Subcontract Number ACI-9-18055-01.
2. The South Coast Air Quality Management District (AQMD) under Contract No. 99157. Under this contract, Clean Air Partners (CAP) served as the prime contractor, with BKM as a subcontractor.

Objective of this project is to develop an enhanced version of Caterpillar C-12 on-highway, heavy-duty, Dual-Fuel truck engine that meets the following requirements: increased rated power and peak torque, retaining the California low NOx and Federal Low Emission Vehicle (LEV) emissions standards, higher gas substitution rates with the same fuel economy relative to the base C-12 Dual-Fuel engine, and potentially a reduction in particulate matter.

This report documents system design, fabrication and experiments conducted in the following task areas:

- Knock detection and control
- Turbo expansion to lower ACT
- Air pressure booster in addition to the stock turbocharger

In order to meet emissions standards originally set for 2004 in October 2002 according to the consent decrees signed in 1998 between EPA, DOJ and engine manufacturers, Caterpillar determined to make a fundamental shift in technological approach. Caterpillar announced on March 6, 2001, a new engine technology for reducing emissions called ACERT™, or Advanced Combustion Emissions Reduction Technology. All Cat® truck engines will employ the ACERT technology, integrated with the next generation HEUI™ fuel system and the latest in electronic engine control. The technologies investigated during this project under both NREL and AQMD contracts have therefore become inappropriate due to the base engine design changes. Commercialization of the technologies as originally envisioned became impossible. It was determined in March 2001, to the interest of all parties concerned, that BKM and CAP should stop work on this project under both contracts.

This final report is prepared and submitted to both NREL and AQMD by CAP in fulfillment of the contracts. This is because effective June 18, 2001, CAP has acquired BKM, resources of CAP and BKM have been consolidated into one entity.

Table of Contents

1	BACKGROUND	1
2	OBJECTIVE	1
3	TECHNICAL APPROACH	1
4	KNOCK DETECTION AND CONTROL	2
4.1	SELECTION OF KNOCK SENSOR	2
4.2	PLACEMENT OF KNOCK SENSORS	3
4.3	CONTROL ALGORITHM DEVELOPMENT	7
5	TURBO COOLING SYSTEM	8
5.1	EFFECT OF REDUCED ACT	11
6	AIR PRESSURE BOOSTER	19
6.1	HYDRAULIC SUPERCHARGER INSTALLATION	19
6.2	HS PERFORMANCE CHARACTERISTICS	22
6.2.1	Full load performance at all engine speeds	22
6.2.2	Performance at constant torque of 1200 lb-ft	23
6.3	DUAL-FUEL ENGINE PERFORMANCE WITH HS	27
6.3.1	Maximum and Minimum Hydraulic Pressure	27
6.3.2	Hydraulic Pressure Modulation	31
6.3.3	Application and Feasibility	35
6.4	OTHER ACTIVITY ON AIR PRESSURE BOOSTER	36
6.4.1	Turbocharger with Smaller A/R Turbine	37
7	SUMMARY AND CONCLUSIONS	42

List of Figures

Figure 1: Knock Sensor for Cylinder #1 and #2	3
Figure 2: Knock Sensor for Cylinder #5 and #6	4
Figure 3: Possible Locations for Cylinder #3 and #4 Knock Sensor	5
Figure 4: Possible Location for Cylinder #3 and #4 Knock Sensor	5
Figure 5: Optimized Knock Sensor Locations	6
Figure 6: Optimized Knock Sensor Locations	6
Figure 7: Controllers Setup for Knock Detection & Control Algorithm Development	7
Figure 8: Turbo Cooling System Installed Upstream of Turbo Compressor	9
Figure 9: Turbo Cooling System Installed Downstream of Turbo Compressor	10
Figure 10: Reducing ACT with Expander	11
Figure 11: Resulting Low Boost with Expander at 1200 rpm	12
Figure 12: EPR of Expander at 1200 rpm	13
Figure 13: Resulting Torque with Expander at 1200 rpm	13
Figure 14: Air Mass Flow with Expander at 1200 rpm	13
Figure 15: Boost and Back Pressure with Expander at 1200 rpm	14
Figure 16: Gas Lambda with Expander at 1200 rpm	14
Figure 17: Pilot Timing with Expander at 1200 rpm	14
Figure 18: Resulting NOx Emissions with Expander at 1200 rpm	15
Figure 19: Engine Output at 1200 rpm, Constant Fuel Delivery	16
Figure 20: NOx Emissions at 1200 rpm, Constant Fuel Delivery	16
Figure 21: CO Emissions at 1200 rpm, Constant Fuel Delivery	16
Figure 22: HC Emissions at 1200 rpm, Constant Fuel Delivery	17
Figure 23: Manifold Pressure at 1200 rpm, Constant Fuel Delivery	17
Figure 24: Air Flow at 1200 rpm, Constant Fuel Delivery	17
Figure 25: Boost and Back Pressure at 1200 rpm, Constant Fuel Delivery	18
Figure 26: Thermal Efficiency at 1200 rpm, Constant Fuel Delivery	18
Figure 27: Expander EPR at 1200 rpm, Constant Fuel Delivery	18
Figure 28: Hydraulic Supercharger Installed on Test Engine	19
Figure 29: Close-up View of the Hydraulic Supercharger	20
Figure 30: Hydraulic Pump Installation	21
Figure 31: Electronic Pressure Regulator – Controlling Turbine Inlet Pressure	21
Figure 32: Air Flow at 100% Load	22
Figure 33: Manifold Absolute Pressure at 100% Load	23
Figure 34: Maximum Hydraulic Turbine Inlet Pressure	24
Figure 35: HS Hyd. Turbine Inlet Pressure Control	24

Figure 36: Air Mass Flow at 1200 lb-ft Torque	25
Figure 37: Manifold Absolute Pressure at 1200 lb-ft Torque.....	25
Figure 38: HS Compressor CPR at 1200 lb-ft Torque.....	26
Figure 39: HS Turbine EPR at 1200 lb-ft Torque	26
Figure 40: Hydraulic Turbine Inlet Pressure Range	27
Figure 41: Maximum Torque Achieved	27
Figure 42: Manifold Absolute Pressure at 100% Load.....	28
Figure 43: Gas Lambda at 100% Load	28
Figure 44: Fuel Delivery at 100% Load.....	28
Figure 45: NOx Emissions at 100% Load	29
Figure 46: HC Emissions at 100% Load	29
Figure 47: CO Emissions at 100% Load	29
Figure 48: ACT at 100% Load.....	30
Figure 49: HS Compression Pressure Ratio at 100% Load.....	30
Figure 50: Max. Torque at Various Hyd. Turbine Pressures.....	31
Figure 51: Boost at Various Hyd. Turbine Pressures.....	31
Figure 52: HS Compressor Inlet Pressure at Various Hyd. Turbine Pressures	32
Figure 53: HS Compressor CPR at Various Hyd. Turbine Pressures.....	32
Figure 54: Boost and Back Pressure Difference at Various Hyd. Turbine Pressures.....	32
Figure 55: HS Air Temperature Increases at Various Hyd. Turbine Pressures	33
Figure 56: Lambda at Various Hyd. Turbine Pressures	33
Figure 57: Thermal Efficiency at Various Hyd. Turbine Pressures	33
Figure 58: NOx Emissions at Various Hyd. Turbine Pressures	34
Figure 59: HC Emissions at Various Hyd. Turbine Pressures	34
Figure 60: CO Emissions at Various Hyd. Turbine Pressures	34
Figure 61: Total Fuel Delivery at Various Hyd. Turbine Pressures.....	35
Figure 62: Overall Compression Pressure Ratio at Full Load.....	37
Figure 63: Max. Torque with 1.28 A/R Turbo	38
Figure 64: Total Fuel Delivery at Full Load with 1.28 A/R Turbo	38
Figure 65: Excess Air Ratio at Full Load with 1.28 A/R Turbo	39
Figure 66: Boost at Full Load with 1.28 A/R Turbo	39
Figure 67: Boost and Back Pressure Difference at Full Load with 1.28 A/R Turbo	40
Figure 68: NOx Emissions at Full Load with 1.28 A/R Turbo.....	40
Figure 69: Thermal Efficiency at Full Load with 1.28 A/R Turbo.....	41
Figure 70: Turbine Inlet Temperature at Full Load with 1.28 A/R Turbo.....	41
Figure 71: Turbine EPR at Full Load with 1.28 A/R Turbo.....	42

Definitions, Acronyms and Abbreviation

ACERT	Advanced Combustion Emissions Reduction Technology
ACT	Air Charge Temperature
AQMD	South Coast Air Quality Management District
A/R	Area to Radius Ratio
BMEP	Brake Mean Effective Pressure
CAN	Controller Area Network
CAP	Clean Air Partners, Inc.
CNG	Compressed Natural Gas
CO	Carbon Monoxide
CPR	Compression Pressure Ratio
DOJ	Department of Justice
ECM	Electronic Control Module
ECU	Engine Control Unit
EPA	Environmental Protection Agency
EPR	Electronic Pressure Regulator
EPR	Expansion Pressure Ratio
FFT	Fast Fourier Transform
HC	Hydrocarbons
HEUI	Hydraulically Actuated Electronically Controlled Unit Injector
HS	Hydraulic Supercharger
LEV	Low Emission Vehicle
LNG	Liquefied Natural Gas
MAP	Manifold Absolute Pressure
MEUI	Mechanically Actuated Electronic Unit Injector
NOx	Nitrogen Oxides
NREL	National Renewable Energy Laboratory
PC	Personal Computer
PM	Particulate Matter
PTO	Power-Take-Off
TAB	Turbo-Air-Bypass
VNT	Variable Nozzle Turbine

1 Background

Due to the nation's continuing concern about energy security and air pollution, Congress enacted the Clean Air Act Amendments of 1990 and the Energy Policy Act (EPACT) of 1992. The provisions of these acts have forced broad changes in fuels and vehicles. For example, reformulated gasoline, clean diesels and alternative fuels are receiving wide attention as industry works to comply with the acts. To meet air quality standards, many of the air quality non-attainment areas across the country will need to increase the use of alternative fuels. Of the major transportation sectors, the heavy-duty vehicles constitute the major increase of US petroleum consumption in the last 10 to 15 years. Using alternative fuels in these vehicles can significantly reduce the US dependence on imported petroleum and also have the potential to greatly reduce particulate and NOx emissions. Natural gas, both compressed (CNG) and liquefied (LNG), has recently emerged as an alternative fuel of choice within the truck and bus sectors. Several heavy-duty engine manufacturers offer dedicated spark-ignited natural gas engines, but their higher cost and lower thermal efficiency limit the use of these products compared to diesel engines.

Dual-Fuel™ natural gas engines retain the diesel compression ratio at over 16:1. At high loads, natural gas that substitutes more than 90% of diesel fuel is introduced with the intake air on the intake stroke. The air and gas mixture is ignited by a small charge of diesel fuel that is injected directly into the cylinder. The Dual-Fuel engine provides the low NOx emissions of a spark-ignited, lean-burn natural gas engine, with the high efficiency and power output of a diesel engine. The base Cat® C-12 Dual-Fuel engine is rated 410-hp and 1250 lb-ft of peak torque. It has the highest rating of any natural gas on-highway engine manufactured. However, a study of fleet operators indicates that 425-hp and 1450 ft-lb of torque are the minimum performance preferred by the majority of commercial fleets. Therefore, with a slight increase in horsepower and torque and a potential for reduction in particulate matter (PM) emissions, the C-12 Dual-Fuel engine could satisfy fleet users as well as air quality advocates.

2 Objective

The goal of this project was to develop an enhanced version of Caterpillar® C-12 on-highway, heavy-duty, Dual-Fuel truck engine with increased rated power and peak torque and the following specifics:

- 425 hp at 1800 rpm and 1450 lb-ft at 1200 rpm
- California low NOx and LEV emission standards
- Higher gas substitution rate
- Maintained fuel economy of the base C-12 Dual-Fuel engine
- Reduced particulate matter emissions compared to the base C-12 Dual-Fuel engine

3 Technical Approach

Both CNG and LNG are known to be vulnerable to fuel quality deterioration. A small drop in fuel octane rating can cause an immediate knock condition. Measures to increase the engine output usually result in an increased tendency to engine knock. An effective anti-knock control system can protect against this event and provide the opportunity to reduce knock safety margins incorporated in the base C-12 Dual-Fuel

engine software. Detecting and controlling engine knock have therefore become essential components of the enhanced C-12 Dual-Fuel engine.

To achieve the LEV rating without compromising efficiency, performance, or other emissions commonly associated with retarded timing for NO_x reduction, an alternative method is required. The effect of air charge temperature (ACT) is well published that lower ACT yields lower NO_x emissions. Lower ACT also reduces knock tendency in Dual-Fuel engines. Cooler air intake temperature therefore allows the brake mean effective pressure (BMEP) to be increased without the risk of knock.

In order to achieve higher torque at 1200 rpm engine speed, the C-12 Dual-Fuel engine requires additional boost air. Excess air ratio (λ) of 1.75 must be maintained for best efficiency, best emissions and protection against knock.

The following technologies were investigated during this project under both NREL and AQMD contracts:

1. Knock detection and control
2. Turbo expansion to lower ACT
3. Air pressure booster in addition to the stock turbocharger

System design, fabrication and experiments conducted on the above technologies are described separately in the following sections of this report.

4 Knock Detection and Control

4.1 Selection of Knock Sensor

Knocking in an internal combustion engine is the uncontrolled self-ignition of the air and fuel mixture occurring midway through the combustion cycle, causing extremely high combustion pressure spikes that destroy pistons and rings in the engine. The knock detection system should be able to detect and analyze the possibility of incipient knock becoming detrimental because of external stress applied to the engine. Engine cylinder bore determines the primary knock frequency, while other dimensions of the combustion chamber, high level harmonics, and the downward motion of the piston control secondary knock frequencies.

Engine combustion analyzer that measures the gas pressure in the combustion chamber in relation to the crankshaft rotational angle is particularly suitable for knock detection. Each cylinder must have an expensive, high temperature pressure transducer installed in the combustion chamber. Modification of cylinder head is required to fit the pressure transducers.

Most automotive manufacturers use one or more accelerometers mounted on the engine block in their production engines. These accelerometers sense high-frequency vibrations generated by knock. The vibration created in the valve train typically run in the same primary frequency range as the knock signal. Base noise levels differ depending on the engine and sensor mounting. The placement of the accelerometers is critical to avoid as much valve train noise as possible and to be as sensitive to the knock vibrations coming from all of the cylinders.

Caterpillar 142-0215 knock sensor was selected on the Enhanced C-12 Dual-Fuel engine for knock detection. This sensor consists of a vibration sensor that changes mechanical vibration into an electrical signal. Decision was made based on the followings:

- The Caterpillar 142-0215 knock sensors are currently used on Caterpillar 3500 gas engines.
- Require less effort on integrating the sensor's electronic control module to the Dual-Fuel truck engine electronic control module (ECM).
- The current Caterpillar 16-Cylinder ECM used on 3516 gas engine is compatible in principle on the Enhanced C-12 Dual-Fuel truck engine with knock detection capability.

4.2 Placement of Knock Sensors

Mounting one sensor for each cylinder is the best guarantee for obtaining sensible signals, although evaluations from one sensor covering two cylinders have also produced reliable results. Caterpillar's experience in mounting this accelerometer type of knock sensor has indicated successful results in using one sensor covering two adjacent cylinders. It was determined that three (3) knock sensors would be directly mounted on engine block at locations closer to the cylinder head gasket.

Instead of using a heat-resistant bonding agent, the Caterpillar 142-0215 knock sensor is fastened on to engine block using M12 thread. Choice of sensor location is therefore restricted by the availability of tapped holes on the engine block currently produced. Figure 1 is the photo taken from a C-12 truck engine showing engine block in way of the Nos. 1 and 2 cylinders. There are two tapped holes available at the left-hand side (camshaft) of the block as indicated by the arrows. One of these holes has the knock sensor installed.

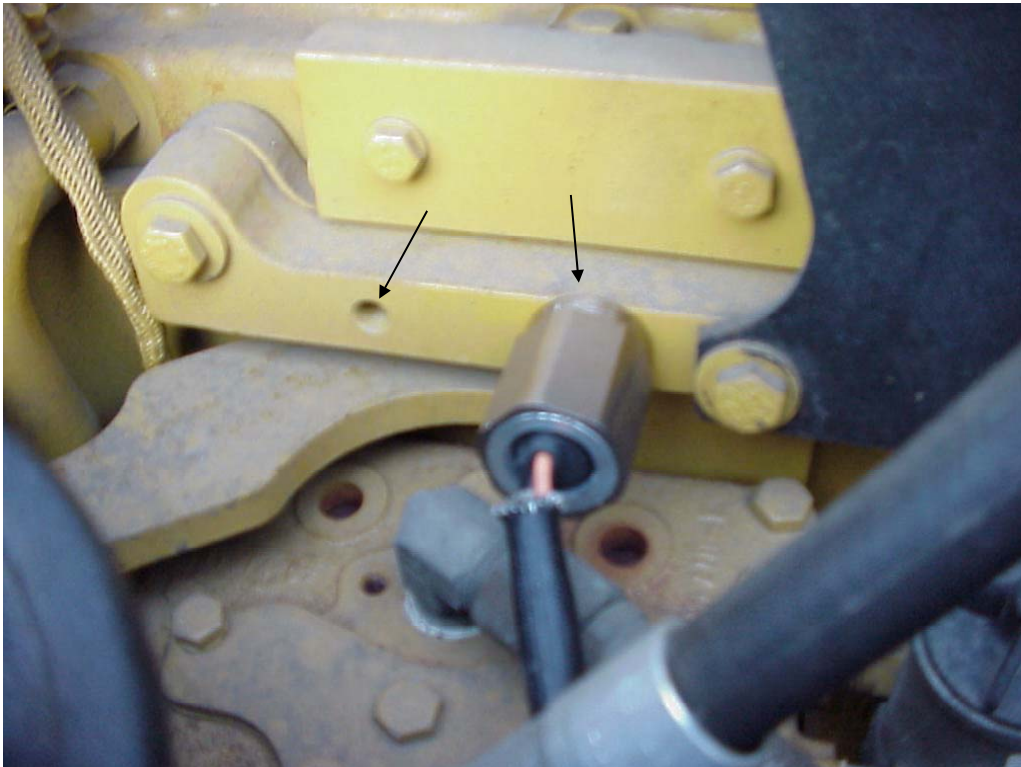


Figure 1: Knock Sensor for Cylinder #1 and #2

Figure 2 is the photo taken from a truck engine showing rear end of engine block where the knock sensor covering cylinder #5 and #6 has been installed. Finding a suitable location for knock sensor covering cylinder #3 and #4 was not so straightforward. Figures 3 and 4 show the possible locations for cylinder #3 and #4 knock sensor.

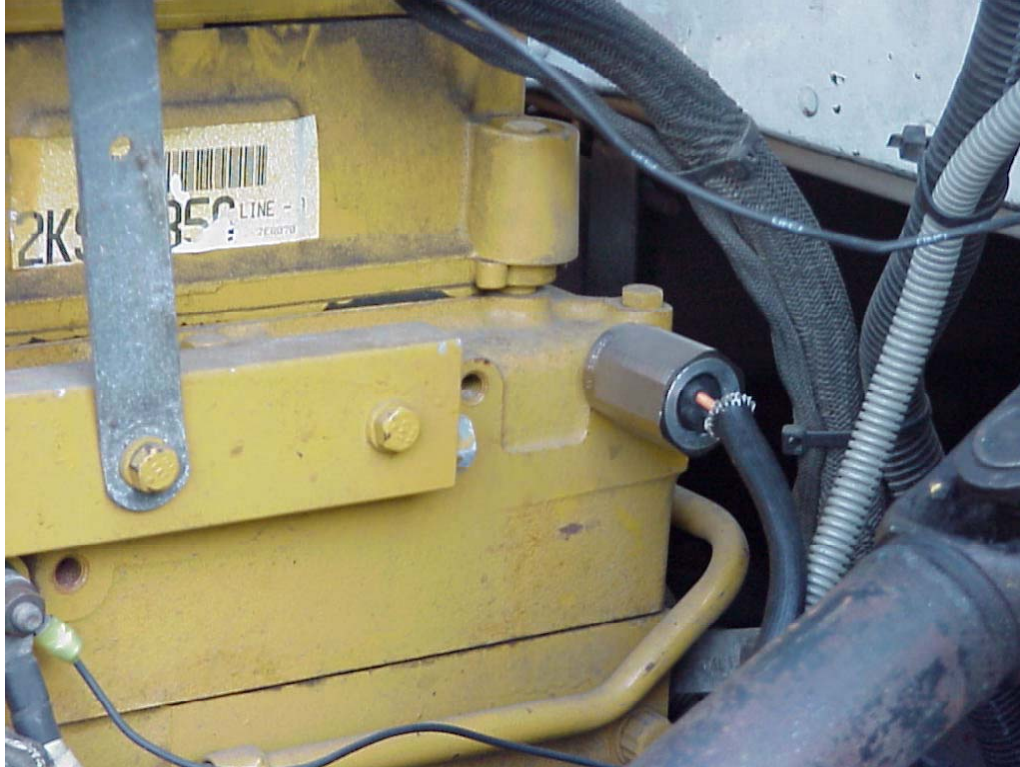


Figure 2: Knock Sensor for Cylinder #5 and #6

The knock-detecting system was installed on the engine in test cell. The system includes three (3) knock sensors and the knock-detecting ECM. Functionality of the system was completely checked out on engine while engine knock was intentionally induced at each designated cylinder by advancing pilot diesel injection timing. Occurrence of Engine knock was verified by using the BKM-built acoustic knock detecting system, and a Kistler in-cylinder pressure transducer that was installed on cylinder #6.

During optimizing the knock sensor location, higher output signal was observed from the front sensor that measures cylinder #1 and #2. It is most likely due to the geartrain noise. Figures 5 and 6 show the optimized location based upon the availability of tapped holes on production engine block. It should not be mistaken that the positioning of knock sensors will not be ideally optimized. Caterpillar will be consulted if additional tapped holes on the engine block become necessary.



Figure 3: Possible Locations for Cylinder #3 and #4 Knock Sensor

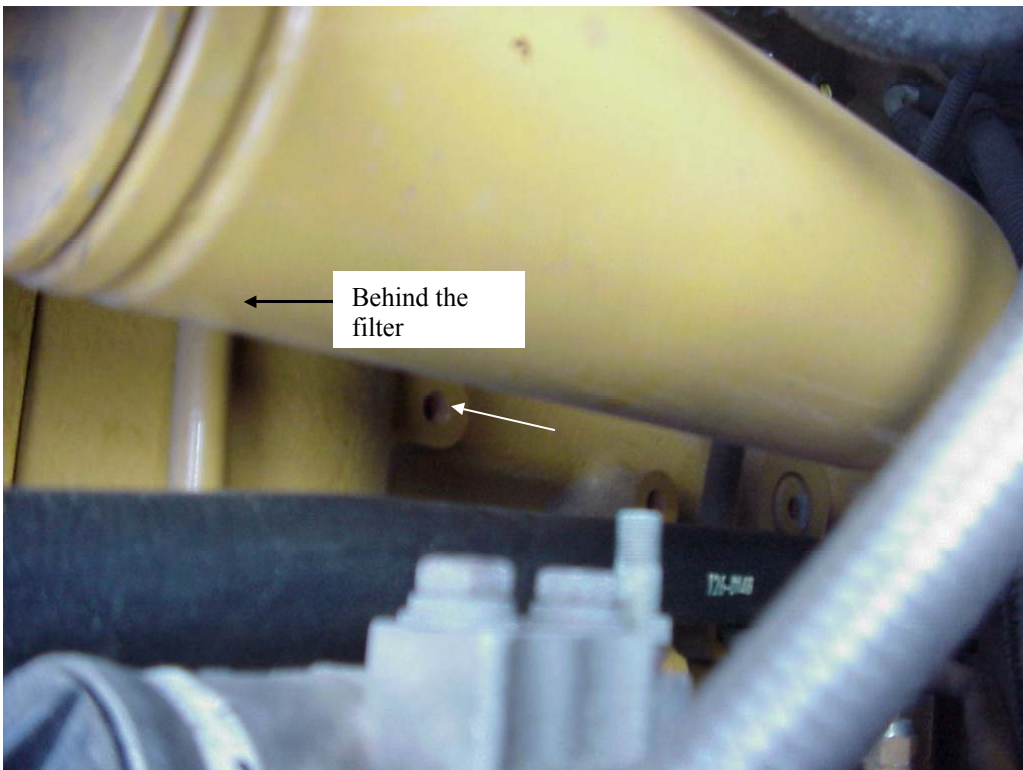


Figure 4: Possible Location for Cylinder #3 and #4 Knock Sensor

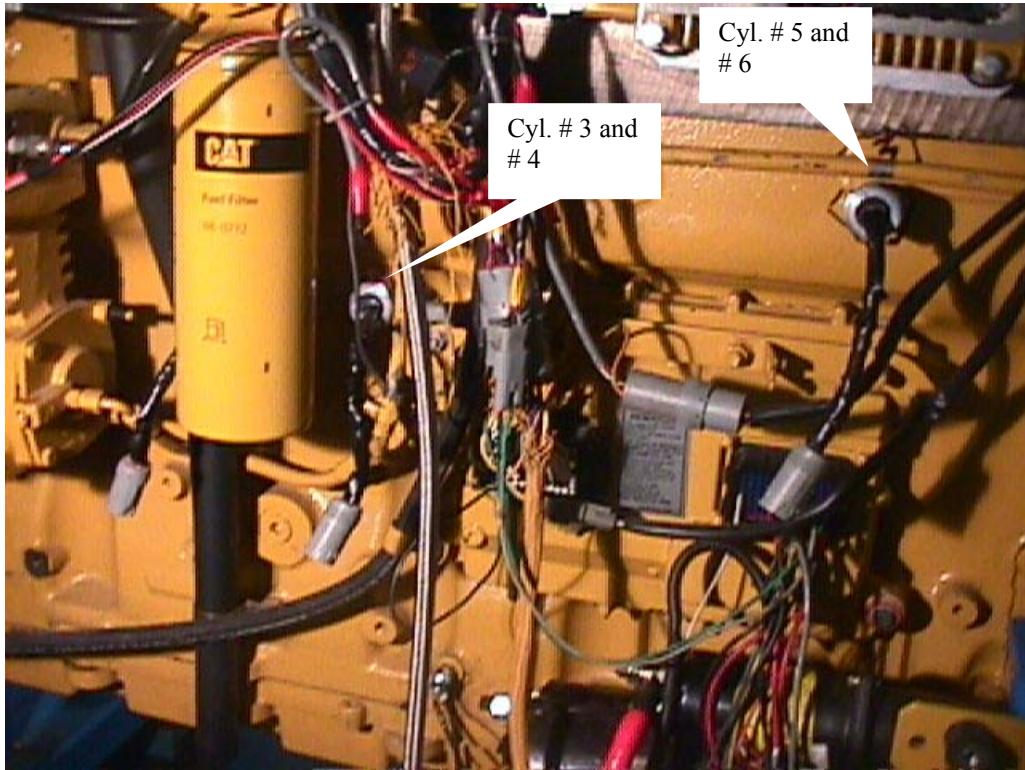


Figure 5: Optimized Knock Sensor Locations

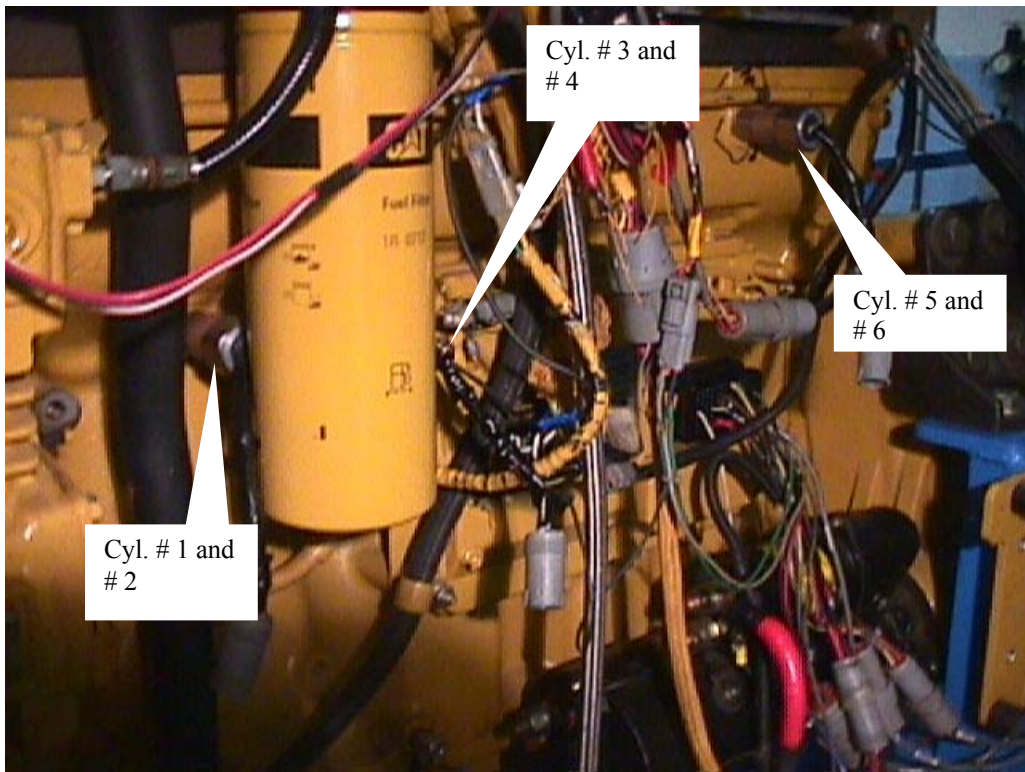


Figure 6: Optimized Knock Sensor Locations

4.3 Control Algorithm Development

Caterpillar's 16-cylinder ECM which is currently used on the 3516 gas engine was selected for knock detecting algorithm development work. This ECM receives signals from three (3) knock sensors, and shares the engine speed/timing signal with the main ECM through J-1939 Controller Area Network (CAN) data link. Once the knock-detecting ECM detects engine knock, the Dual-Fuel engine control unit (ECU) that controls and governs the Dual-Fuel operation will immediately be prompted, and correction measures will be taken. Three electronic controllers were used during the knock detection and control development. Figure 7 shows the setup of controllers for knock detection and control algorithm development.

Software for this knock-detecting ECM was developed. Knock sensor signals were monitored within a programmable crank angle based window for each individual cylinder. This method allows interference noise to be eliminated. A 4~20 mA analog output signal was sent to the Dual-Fuel ECU whenever engine knock was detected from any one of the three sensors. This signal indicated the specific cylinder that knocked as well as the intensity of knock.

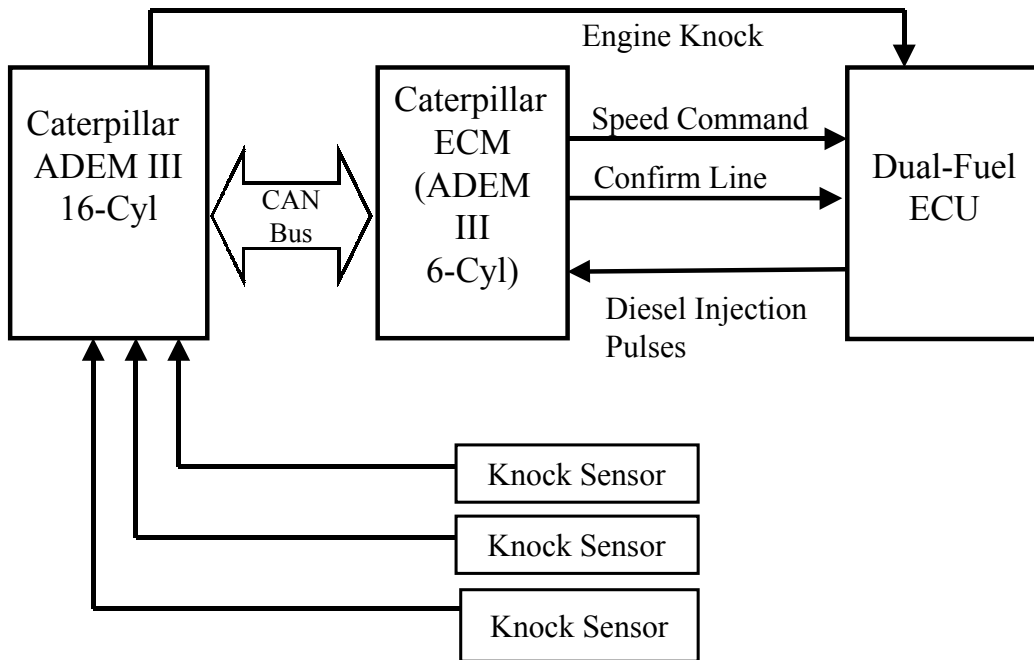


Figure 7: Controllers Setup for Knock Detection & Control Algorithm Development

Software for the current production Caterpillar ECM was also modified so that pilot diesel timing could be adjusted on each individual cylinder from Cat engine development tool through communication adapter and PC. Intentional knock could therefore be generated at each designated cylinder and verified by the acoustic knock detecting system during the development work in test cell.

A standard production Dual-Fuel ECU was modified to receive the 4~20 mA analog signal. Once the knock-detecting ECM detects engine knock, the Dual-Fuel ECU that controls and governs the Dual-Fuel operation will be notified. Knock control strategies

such as retarding pilot diesel timing, reducing gas delivery and increasing excess air ratio, were established.

In order to have an accurate indication of engine knock from these block-mounted knock sensors, separating the knock signal from the vibrations from valve train, crankshaft and pistons is needed. As mentioned on section 4.1 that engine cylinder bore determines the primary knock frequency, while other dimensions of the combustion chamber, high level harmonics, and the downward motion of the piston control secondary knock frequencies, each engine would have different frequency characteristics. The knock detecting hardware which was derived from that used on Caterpillar 3512 gas engine, might not be perfectly suitable for the C-12 Dual-Fuel engine. Frequency analysis on knock sensor signals recorded was performed using Fast Fourier Transform (FFT) techniques. Several amplitude spectrum plots indicated the optimum frequency band for knock detection was approximately 20 ~ 25 kHz for C-12 Dual-Fuel engine. A new knock-detecting ECM having 20 ~ 25 kHz band-pass filter was then assembled.

Testing of knock-control algorithm was not completed when the project stopped in February 2001.

5 Turbo Cooling System

The effect of air charge temperature (ACT) is well published that lower ACT yields lower NO_x emissions. Lower ACT also reduces knock tendency in Dual-Fuel engines. Cooler air intake temperature therefore allows the BMEP to be increased without the risk of knock. This task was originally proposed to lower the ACT with the incorporation of turbo expander. It was proposed that lowering ACT would reduce NO_x emission further, enough to advance the pilot diesel timing for increased torque while keeping NO_x emission below 2.5 g/hp-h.

Low ACT, well below ambient, can be achieved by adding a turbo cooling system to the existing air intake system. The turbo cooling system consists of a compressor (blower) driven by an air-turbine and an intercooler. This unit can be installed either upstream or downstream of the existing turbocharger as shown on Figures 8 and 9.

Refer to Alternative 2 shown in Figure 9, the intake air is pressurized by the turbocharger blower and cooled by the intercooler in the same way as a conventional system. The compressed and cooled air is re-pressurized by the compressor driven by the air-turbine, and cooled by the intercooler. The high pressure, low temperature air is then expanded and cooled further with the turbine.

Using the diesel baseline engine test data at peak torque (1200 rpm engine speed and 1450 ft-lb torque), a parametric study on the air intake system turbo expander was performed. Appendix 1 includes the parametric study results which are summarized below:

1. Optimized turbo expander characteristics at peak torque:
Expansion pressure ratio (EPR) of air turbine: 1.80
Compression pressure ratio (CPR) of compressor: 1.50
2. The turbo expander intercooler shall be at least 50% as effective as the existing exhaust turbocharger air-to-air intercooler.
3. ACT of 5 °C will yield an excess air ratio of 1.7 at peak torque.

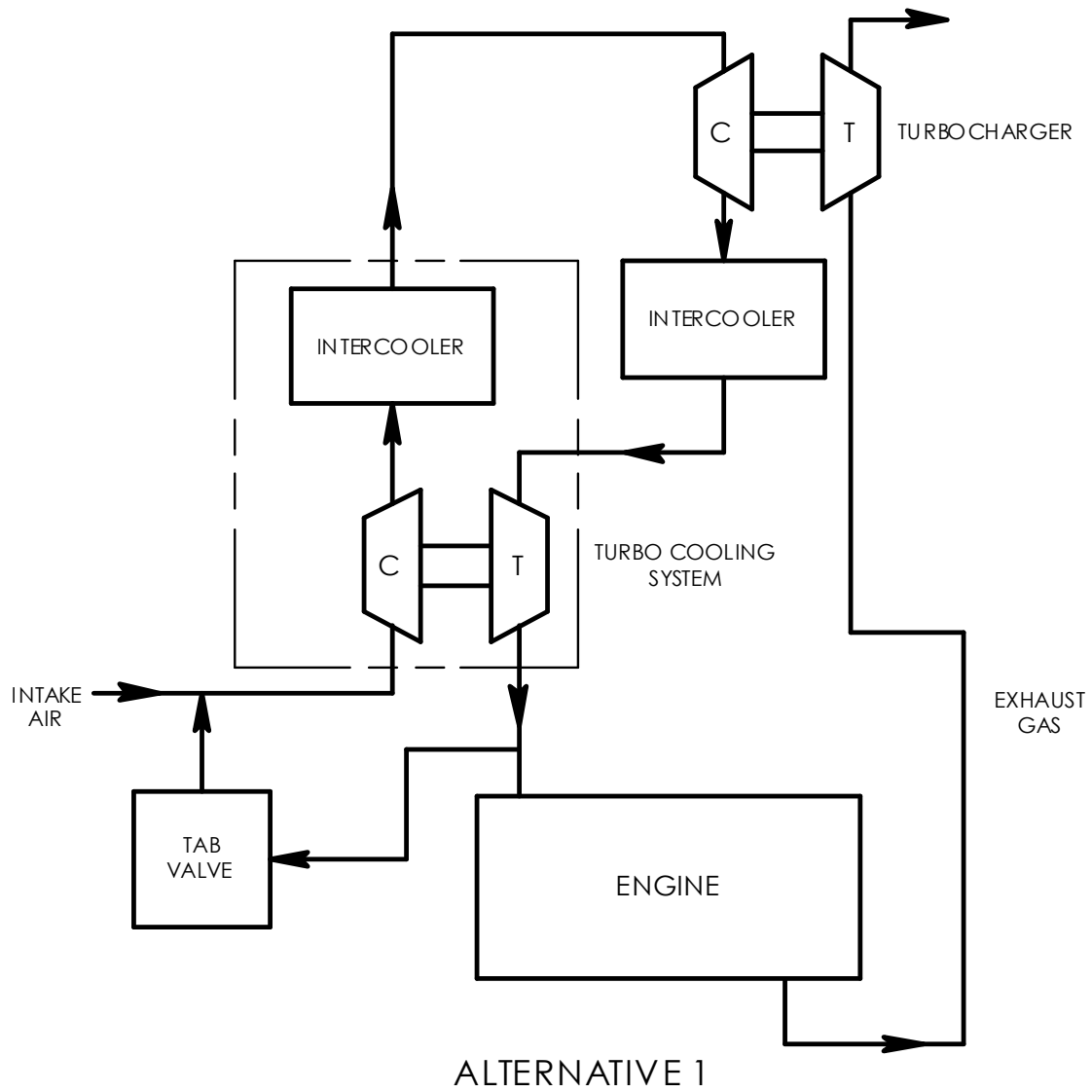
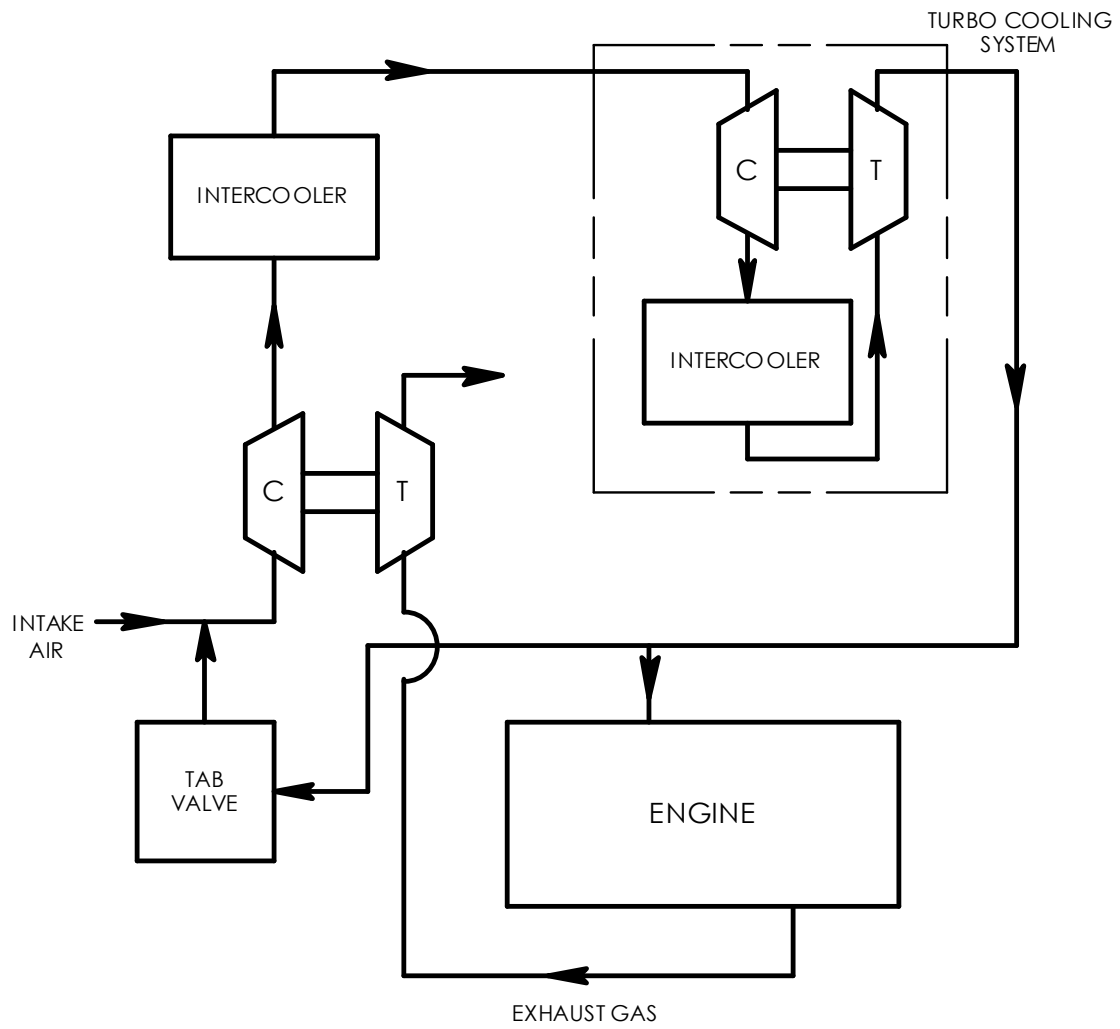


Figure 8: Turbo Cooling System Installed Upstream of Turbo Compressor



ALTERNATIVE 2

Figure 9: Turbo Cooling System Installed Downstream of Turbo Compressor

5.1 Effect of Reduced ACT

Prior to continuing the characterization of the turbo expander requirements for the entire engine operation range, a feasibility study was conducted to determine the effect of reduced ACT on NO_x emissions. A commercial air chiller for intake air cooling was planned. Proposals received indicated that the chiller application within the test cell environment was not practical due to the additional floor space and electrical power required.

A Turbonetics' T-4 turbocharger was used as an alternate method to evaluate the effect of reduced ACT. The T-4 turbine has 0.6 area to radius ratio and an expansion pressure ratio of 1.5. The T-4 turbine was connected in series with the intercooler outlet and feeding the normal intake manifold. The T-4 compressor inlet was open to atmosphere. A manual operated butterfly valve was installed at the compressor outlet for turbine load if required. ACT reduction of 20 °C was anticipated. Figure 10 shows the schematic diagram of the air intake system.

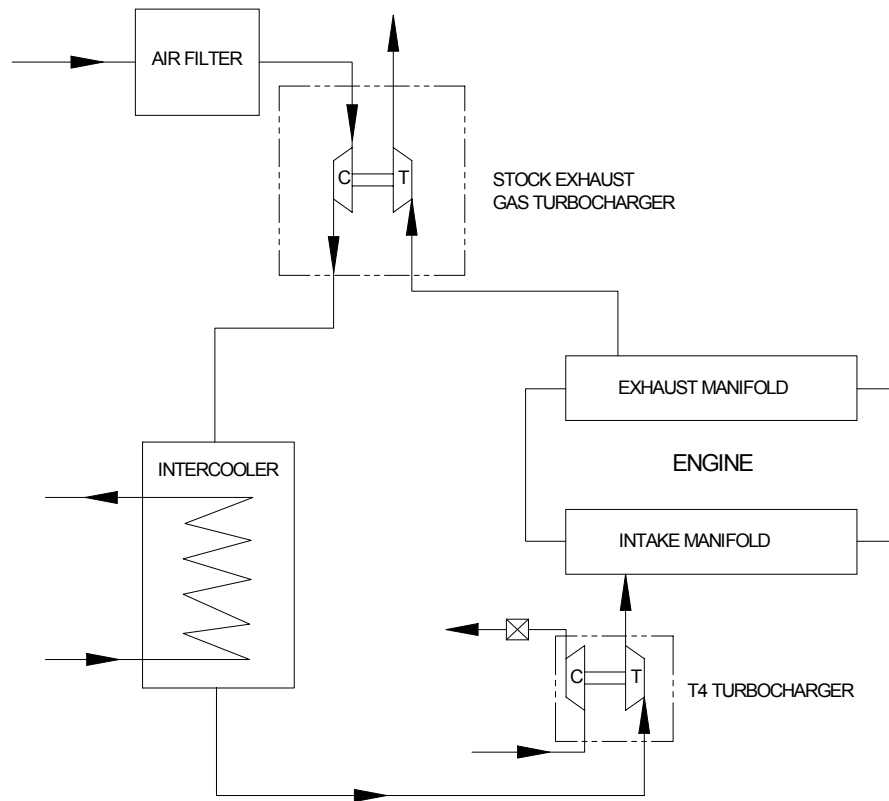


Figure 10: Reducing ACT with Expander

Initial engine test was performed to evaluate the effect of reduced ACT at a constant engine speed of 1200 rpm.

The following summarizes the test results and findings:

1. Boosted air leaving the exhaust gas turbocharger and intercooler was expanded at the T-4 turbine. Manifold absolute pressure (MAP) of 89 kPa was observed at idle and 101 kPa barometric pressure. ACT was reduced by 15 °C. Cooling water passing through the air-to-water intercooler was gradually reduced to increase the ACT to 40 °C during the test. Figures 11 and 12 show MAP and expansion pressure ratio, respectively, at various ACT.
2. The engine with reduced boost and ACT was able to produce 500 ~ 550 ft-lb torque as shown in Figure 13. A reduction of 50% comparing to the base C-12 Dual-Fuel engine.
3. Less air was being forced into the cylinder, as the exhaust back pressure was 15 kPa higher than the intake pressure. Figures 14 and 15 show air mass flow and pressure difference between exhaust and intake.
4. The preliminary results indicated that reduced ACT has no significant effect on emissions at 50% load. Gas lambda and pilot timing are the dominating parameters that affect NOx emissions. Figure 16 shows that gas lambda ranging from 1.32 ~ 1.38 was maintained at various ACT. Pilot timing and NOx emissions are plotted against ACT as shown in Figures 17 and 18, respectively.

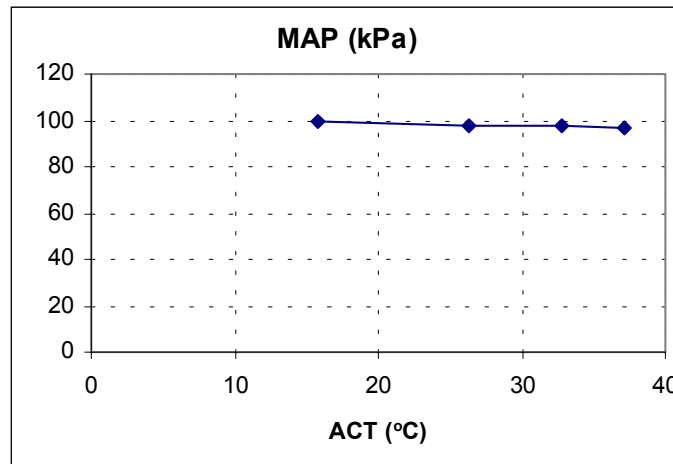


Figure 11: Resulting Low Boost with Expander at 1200 rpm

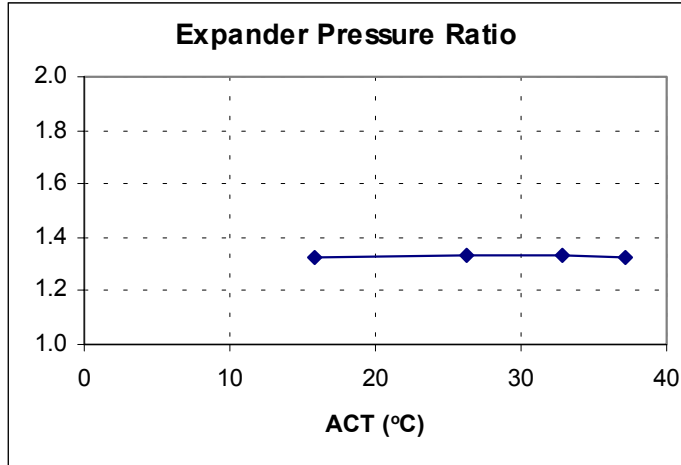


Figure 12: EPR of Expander at 1200 rpm

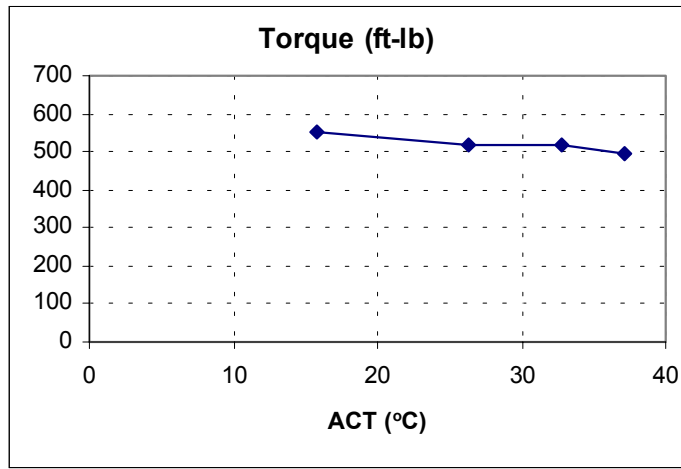


Figure 13: Resulting Torque with Expander at 1200 rpm

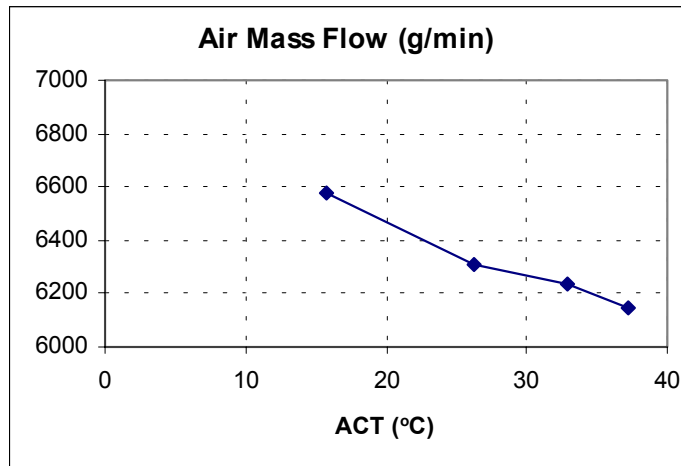


Figure 14: Air Mass Flow with Expander at 1200 rpm

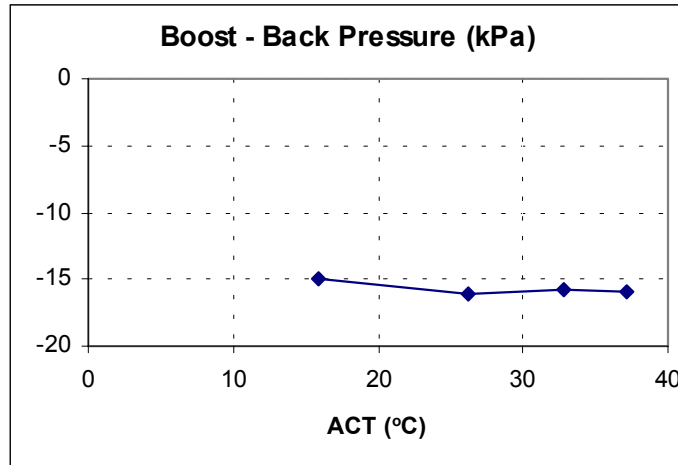


Figure 15: Boost and Back Pressure with Expander at 1200 rpm

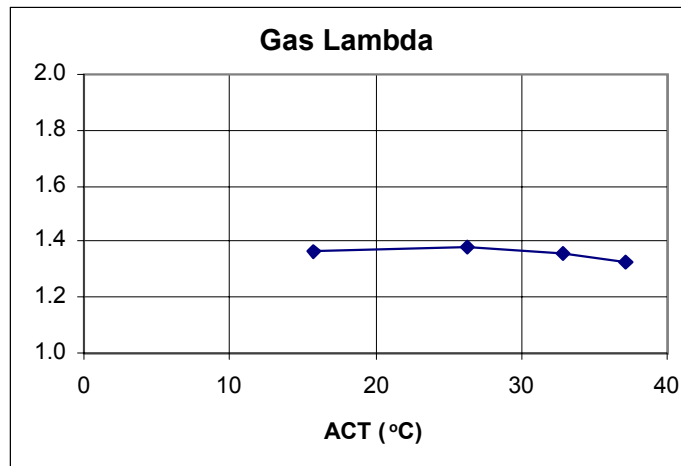


Figure 16: Gas Lambda with Expander at 1200 rpm

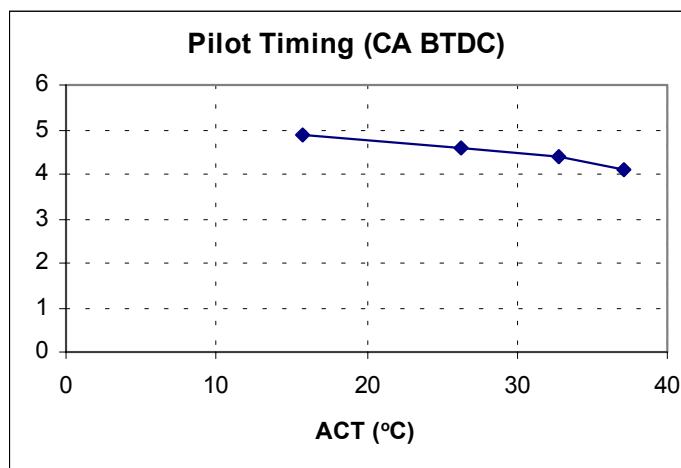


Figure 17: Pilot Timing with Expander at 1200 rpm

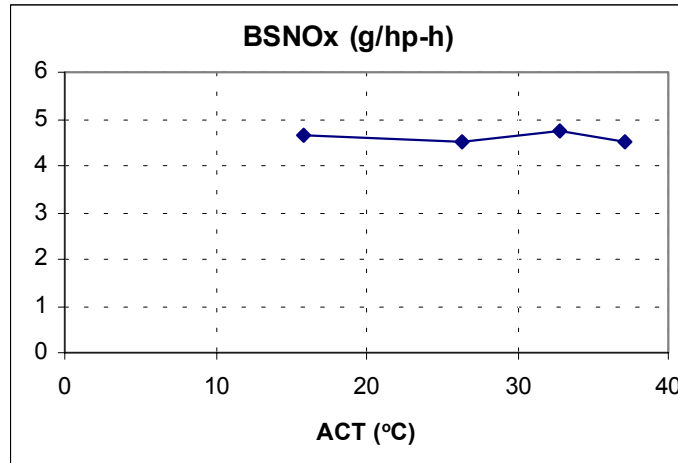


Figure 18: Resulting NOx Emissions with Expander at 1200 rpm

In order to investigate the reduced ACT effect closely at a constant engine speed of 1200 rpm, more engine tests were conducted at constant total fuel delivery as described below:

1. Speed and load were maintained at 1200 rpm and 460 lb-ft, respectively.
2. Commanded fuel was kept constant at 100 mm³/cyl diesel equivalent.
3. Pilot diesel delivery was maintained at 18.6 mm³/cyl.
4. Gas delivery to each cylinder was maintained at 63 mg.
5. Turbo Air Bypass (TAB) valve located upstream of the turbine expander was used to vary gas lambda from 1.25 to 1.50, while keeping ACT constant.
6. Varied ACT from 15 °C ~ 40 °C by regulating water flow through the air-to-water aftercooler, while keeping lambda constant.

Engine parameters were plotted against lambda at various ACT as shown in Figures 19 ~ 27 below. Test results are summarized as follow:

1. For lean-burn Dual-Fuel engine, ACT does not affect performance and emissions characteristics significantly, for given lambda.
2. Unlike diesel engine, the lean-burn Dual-Fuel engine has total control of lambda which makes ACT have no effect on performance and emissions.
3. Gas lambda is a dominating factor on performance and emissions.
4. NOx emission decreases from 6 g/hp-h to 3.5 g/hp-h while gas lambda increases from 1.25 to 1.50.
5. Thermal efficiency is not affected by ACT.

Development effort on the complete turbo cooling system to lower ACT as shown in Figure 9 was therefore ceased based on the above findings.

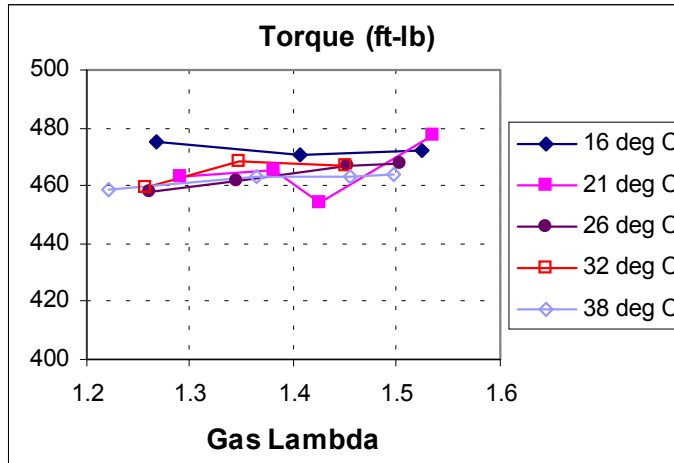


Figure 19: Engine Output at 1200 rpm, Constant Fuel Delivery

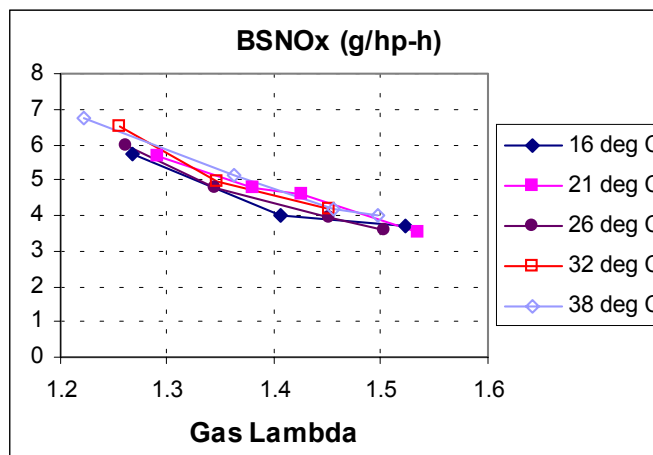


Figure 20: NOx Emissions at 1200 rpm, Constant Fuel Delivery

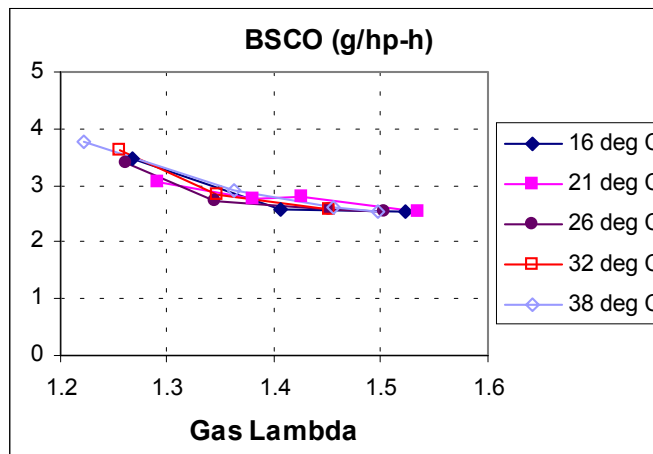


Figure 21: CO Emissions at 1200 rpm, Constant Fuel Delivery

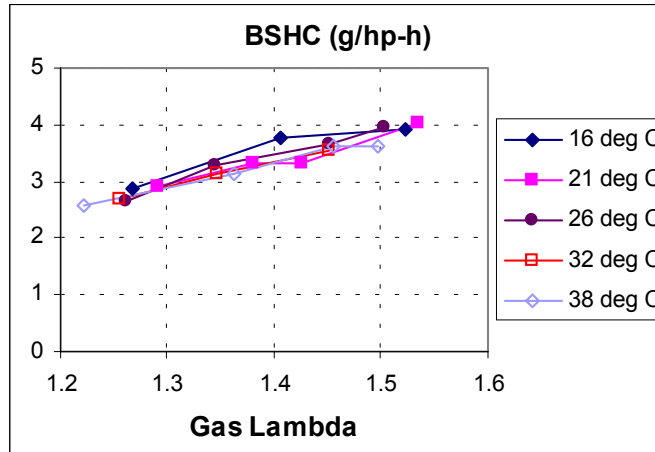


Figure 22: HC Emissions at 1200 rpm, Constant Fuel Delivery

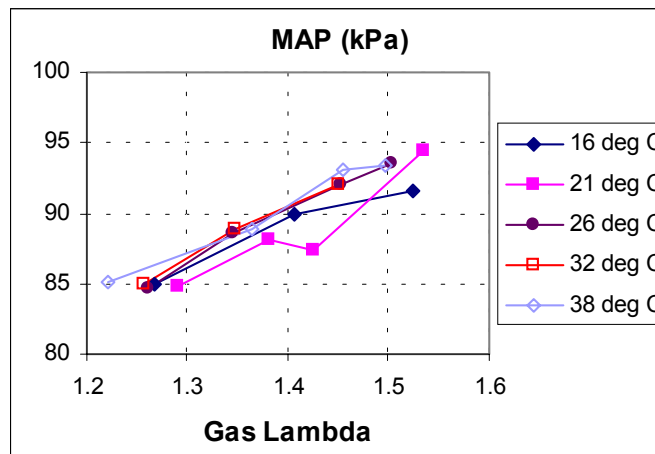


Figure 23: Manifold Pressure at 1200 rpm, Constant Fuel Delivery

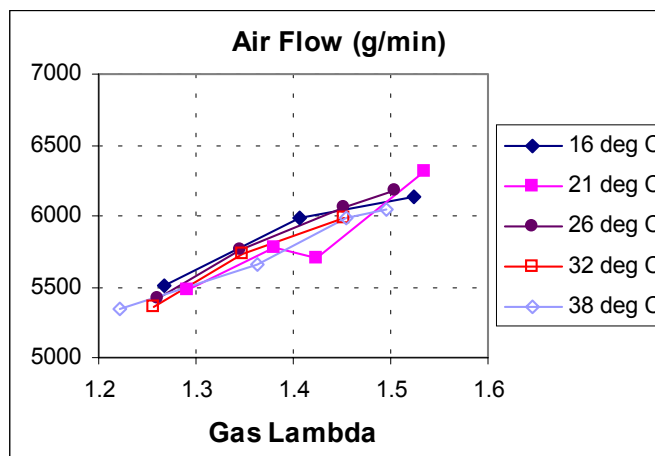


Figure 24: Air Flow at 1200 rpm, Constant Fuel Delivery

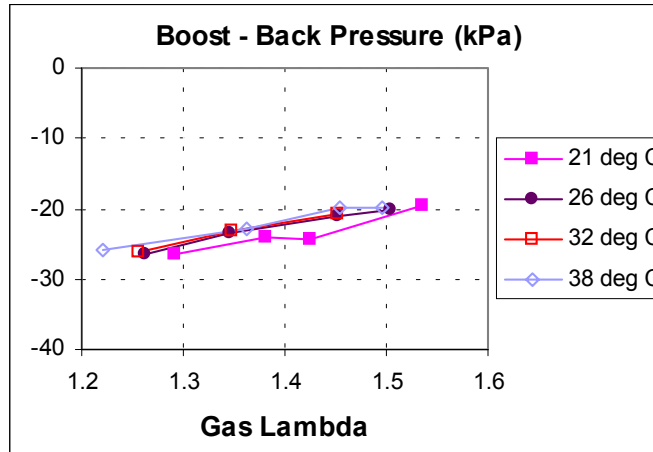


Figure 25: Boost and Back Pressure at 1200 rpm, Constant Fuel Delivery

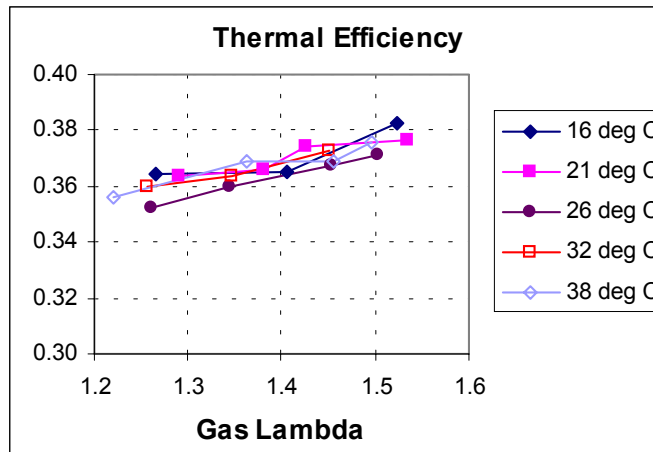


Figure 26: Thermal Efficiency at 1200 rpm, Constant Fuel Delivery

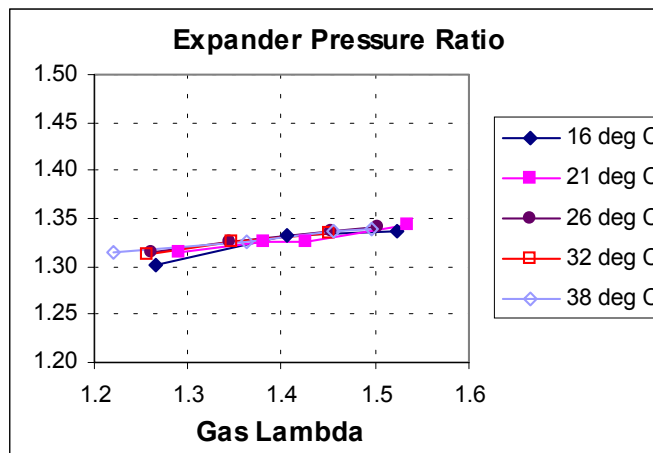


Figure 27: Expander EPR at 1200 rpm, Constant Fuel Delivery

6 Air Pressure Booster

The base C-12 Dual-Fuel engine retains the stock turbocharger originally matched for diesel operation. The C-12 Dual-Fuel engine requires more air charge than that is needed by diesel engine at engine speed below 1400 rpm, to maintain the optimum air/fuel ratio for best efficiency and emissions. Therefore, peak torque of the base C-12 Dual-Fuel engine is rated lower than the diesel engine. In order to achieve higher torque at low engine speeds, turbocharger incorporated with a variable nozzle turbine (VNT) will be the best solution. When the proposal was made to NREL and AQMD, VNT turbocharger intended for heavy-duty highway truck diesel engines in the 12 ~ 14 liters displacement range was not known. The Kapich hydraulic supercharger was the known available component that would provide a straightforward way to achieve added boost.

6.1 Hydraulic Supercharger Installation

The hydraulic supercharging system consists of the following components:

1. Kapich hydraulic supercharger (HS) that consists of GHC10-18 hydraulic turbine and TA-97 compressor
2. Sundstrand SP2.5/250-45 hydraulic pump, 45 cc/rev.
3. Wandfluh proportional pressure control valve

The Kapich HS was installed downstream of the exhaust turbocharger aftercooler as shown in Figures 28 and 29.

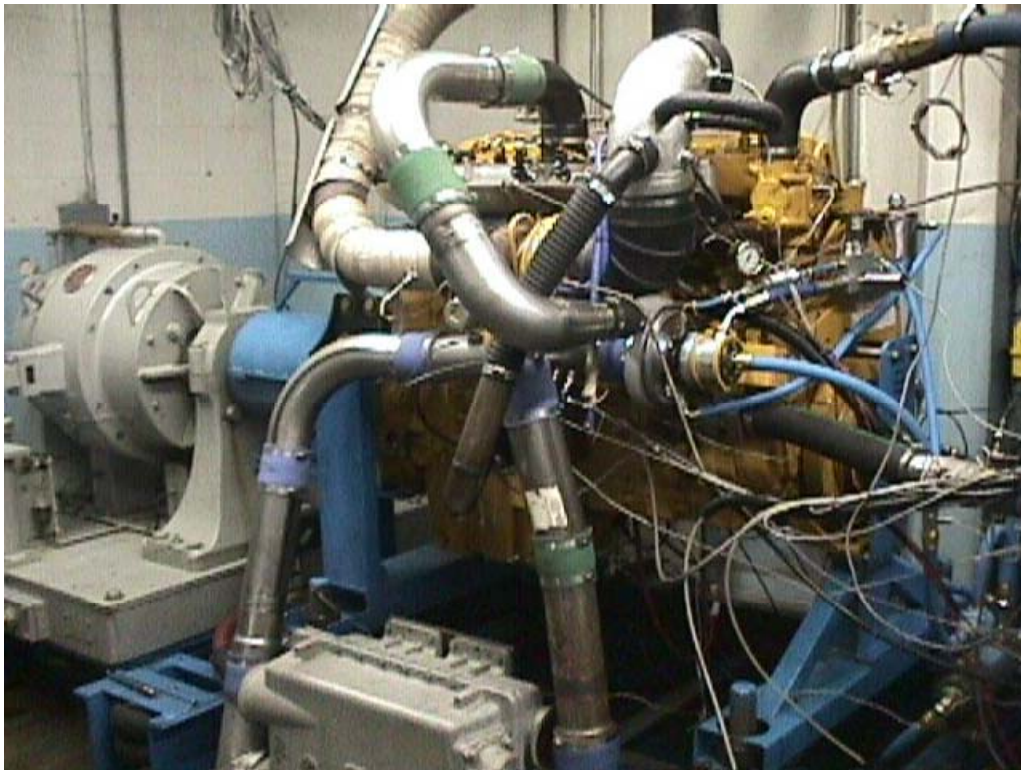


Figure 28: Hydraulic Supercharger Installed on Test Engine



Figure 29: Close-up View of the Hydraulic Supercharger

The hydraulic pump was coupled on to the PTO shaft and driven at 48/34 engine speed as shown in Figure 30.

A Wandfluh proportional pressure control valve was used to regulate the hydraulic turbine inlet turbine as shown in Figure 31. The proportional solenoid was pulse-width-modulated (PWM) at 400 Hz by a separated controller during the test and evaluation on engine dyno. Varying the turbine inlet pressure would change the compressor performance characteristics, i.e., compression pressure ratio vs air mass flow. Incorporating the closed-loop control of turbine inlet pressure on the existing Dual-Fuel ECU was planned upon completion of laboratory testing.

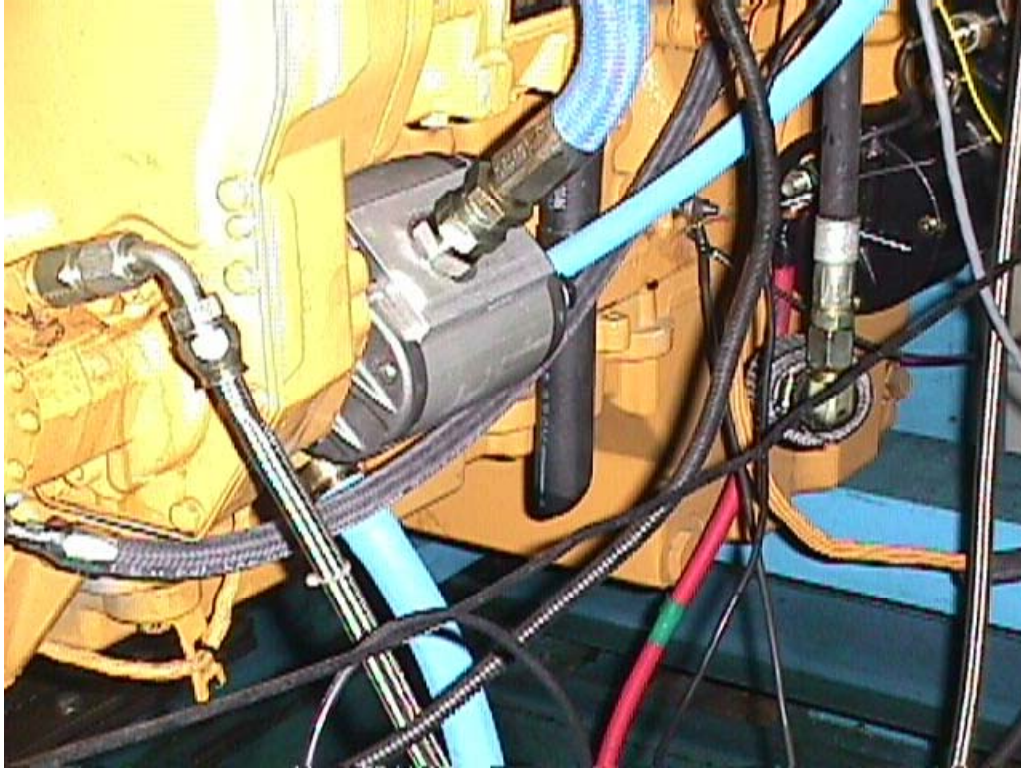


Figure 30: Hydraulic Pump Installation



Figure 31: Electronic Pressure Regulator – Controlling Turbine Inlet Pressure

6.2 HS Performance Characteristics

Performance characteristics of the HS was evaluated by running the C-12 Dual-Fuel engine in test laboratory on 100% diesel fuel operation.

Data obtained from engine test with the HS was thoroughly analyzed and compared with that obtained from the diesel baseline test. The following sections summarize the performance characteristics of the Kapich hydraulic supercharger:

6.2.1 Full load performance at all engine speeds

Performance of the HS was evaluated at all engine speeds and maximum fuel rack.

Figure 32 illustrates the air mass flow capability of the HS at all speeds and 100% load. Hydraulic turbine that drives the supercharger is running at maximum supply pressure available from the engine driven pump. It is evident that air mass flow increases at all engine speeds when the HS is employed. It is note-worthy that the current base C-12 Dual-Fuel engine employs Turbo Air Bypass (TAB) valve to bleed excessive air delivered by the original turbocharger for optimum lambda, at engine speeds above 1600 rpm. In other words, additional air mass flow is only required at engine speeds below 1300 rpm for the enhanced C-12 Dual-Fuel engine.

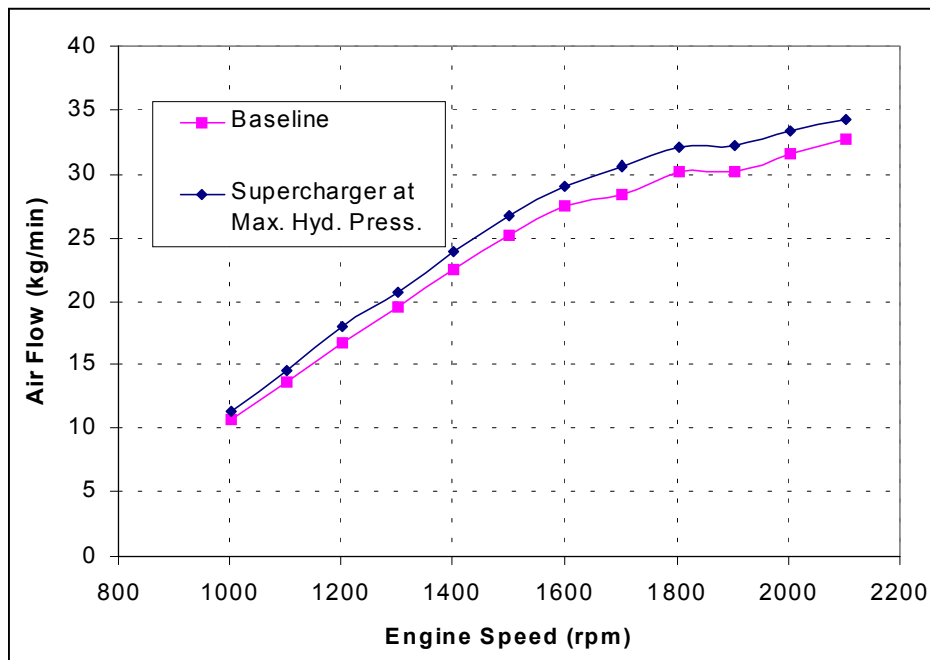


Figure 32: Air Flow at 100% Load

MAP which is commonly known as turbo boost pressure is plotted against engine speed at full loads as shown in Figure 33. MAP exceeds 300 kPa at engine speeds between 1500 ~ 1800 rpm, when the HS is operated at maximum hydraulic turbine inlet pressure.

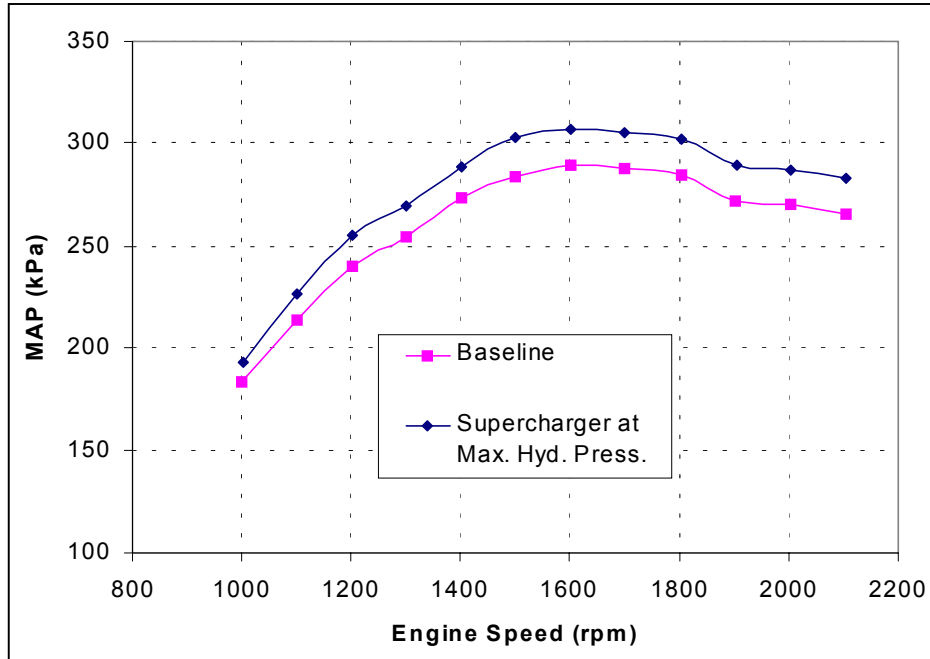


Figure 33: Manifold Absolute Pressure at 100% Load

As mentioned on Section 6.1, the hydraulic pump which is a positive displacement pump, was driven at 48/34 engine speed. An electronic pressure regulator that consists of a Wandfluh proportional pressure control valve was used to regulate the hydraulic turbine inlet pressure. When the proportional solenoid was PWM at 100% duty cycle, the hydraulic turbine received maximum pressure that the pump could provide. All full load data was taken with 100% duty cycle to evaluate the capability of the HS. Figure 34 shows the maximum HS hydraulic turbine inlet pressure at all engine speeds.

6.2.2 Performance at constant torque of 1200 lb-ft

It is well known that "torque rise" is one of the important characteristics of a heavy-duty truck engine. Performance of the HS was evaluated at a constant torque of 1200 lb-ft and engine speeds of 1200, 1400 and 1600 rpm. At each engine speed, while engine was loaded at a constant torque of 1200 lb-ft on an engine dyno, the HS electronic pressure regulator was set at five different settings, i.e., 0, 70, 80, 90 and 100% duty cycle. The 0% duty cycle setting yields the minimum hydraulic turbine inlet pressure, while 100% duty cycle setting allows the maximum pressure that the pump can provide. The hydraulic turbine inlet pressure is plotted against the HS EPR duty cycle at 1200, 1400 and 1600 rpm as shown in Figure 35. It is evident that with the current HS configuration, the hydraulic turbine inlet pressure control is limited within a rather small EPR duty cycle range, i.e., 70 ~ 100%. The hydraulic turbine inlet pressure that can be regulated is also very small, i.e., 31 psi at 1200 rpm, 48 psi at 1400 rpm and 64 psi at 1600 rpm. In other words, the EPR control has a large dead-band (0 ~ 70%), and the pressure regulation is less than $\pm 9\%$ of the nominal pressure.

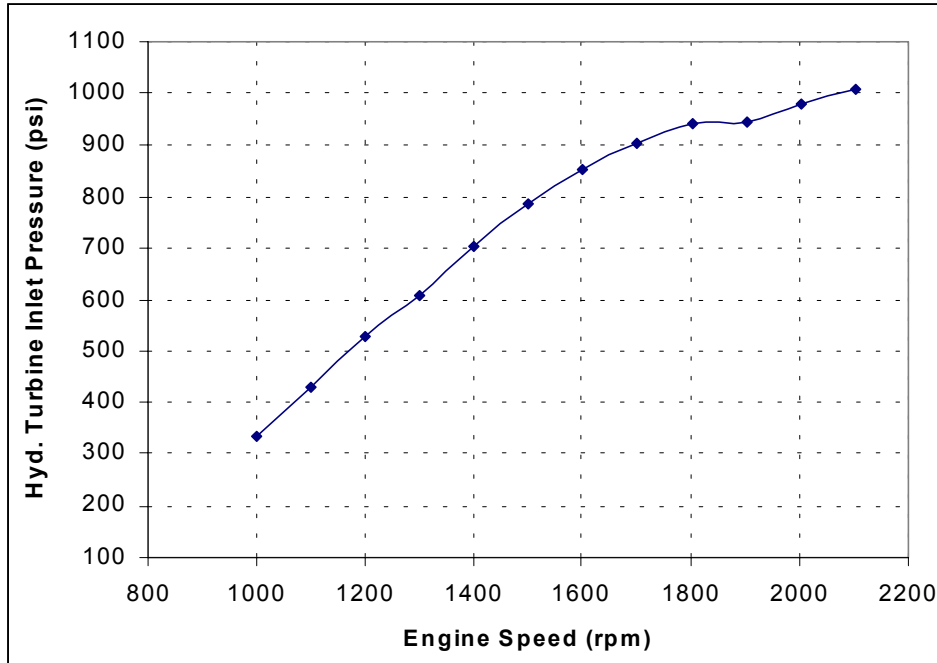


Figure 34: Maximum Hydraulic Turbine Inlet Pressure

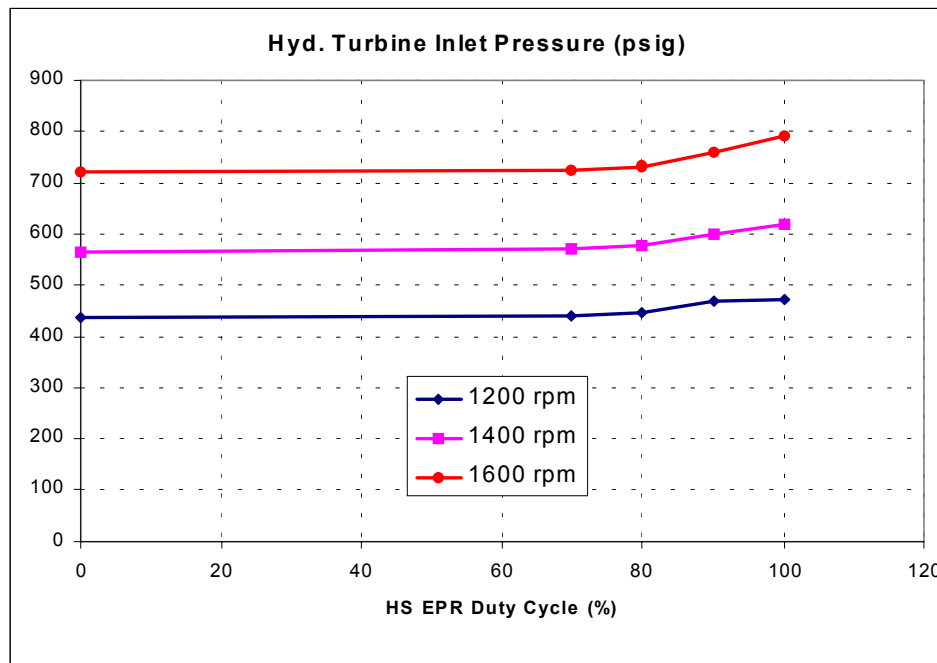


Figure 35: HS Hyd. Turbine Inlet Pressure Control

Figure 36 shows the resulting air mass flow at a constant torque of 1200 lb-ft, 1200, 1400 and 1600 rpm, while the HS EPR was set at 0, 70, 80, 90 and 100% duty cycle.

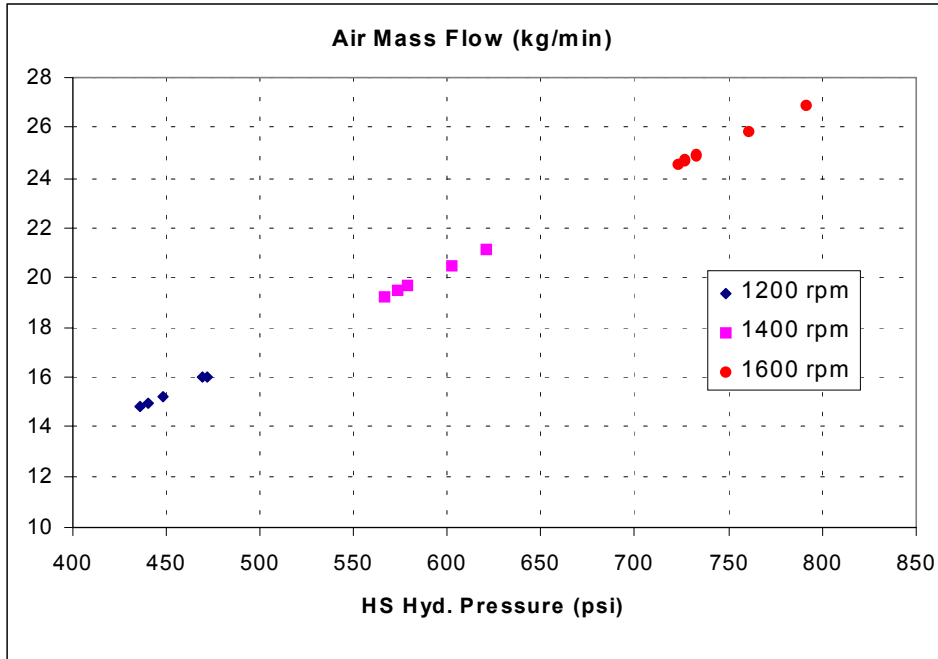


Figure 36: Air Mass Flow at 1200 lb-ft Torque

MAP, HS compressor CPR and turbine EPR are plotted against the regulated hydraulic turbine inlet pressure as shown in Figures 37 ~ 39, respectively.

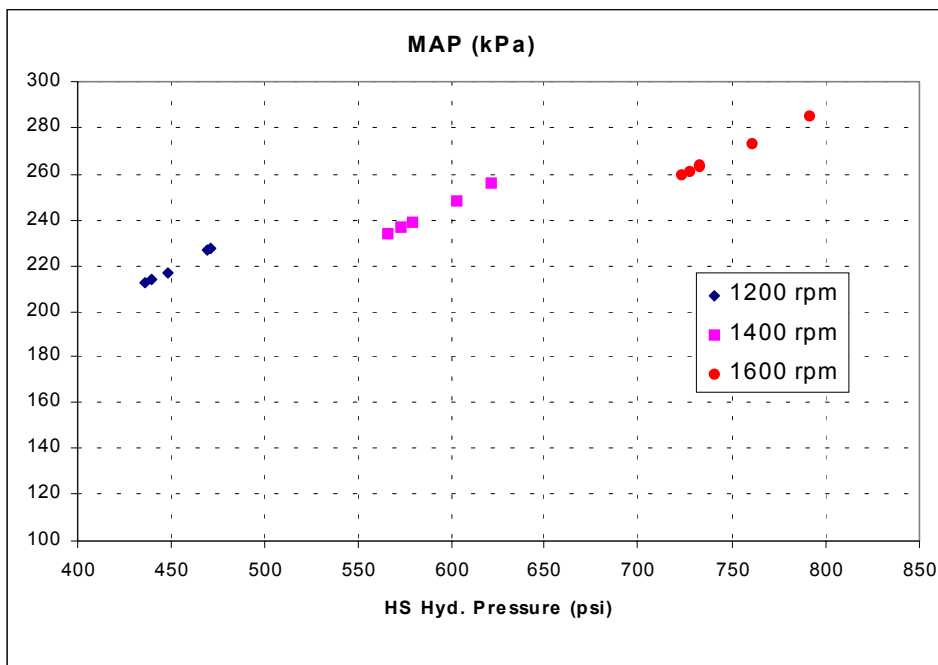


Figure 37: Manifold Absolute Pressure at 1200 lb-ft Torque

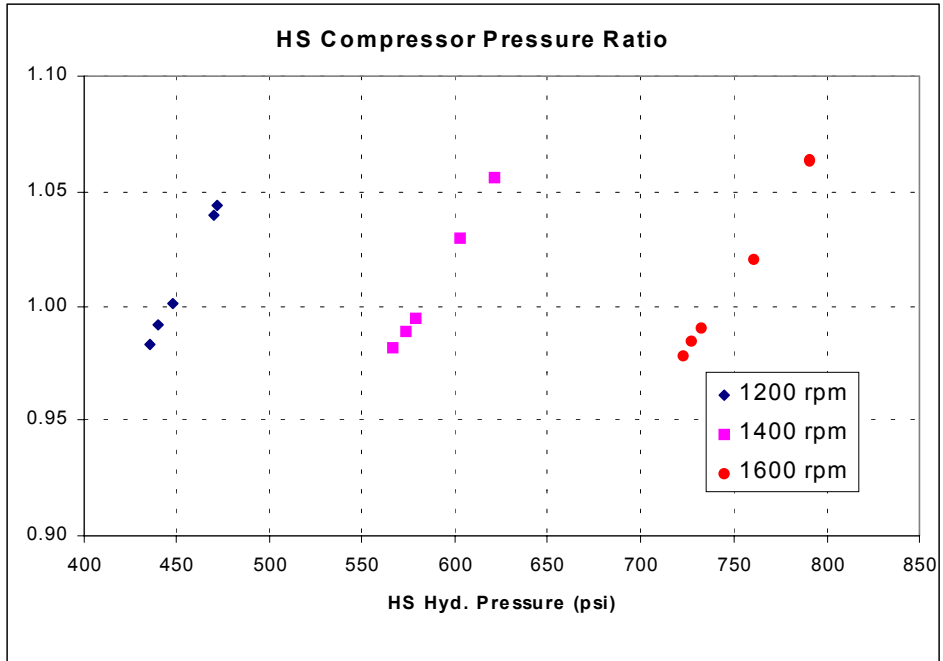


Figure 38: HS Compressor CPR at 1200 lb-ft Torque

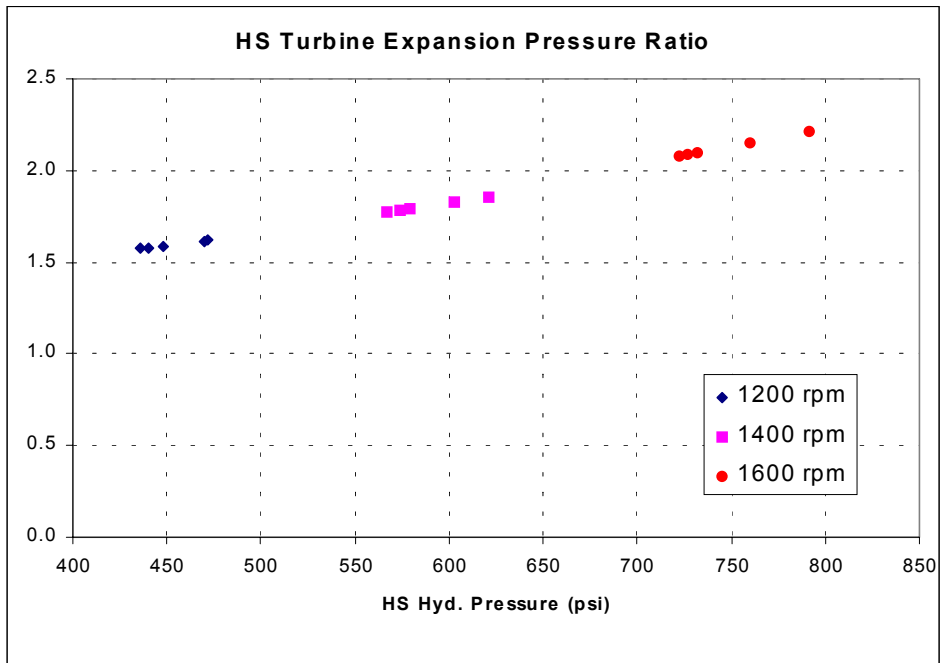


Figure 39: HS Turbine EPR at 1200 lb-ft Torque

6.3 Dual-Fuel Engine Performance with HS

Once performance of the hydraulic supercharger was characterized on 100% diesel fuel, testing and evaluation of the HS on dual-fuel operation was commenced, focusing at engine speeds ranging from 1000 ~ 1500 rpm, as additional boost is not required at engine speeds above 1500 rpm.

6.3.1 Maximum and Minimum Hydraulic Pressure

The C-12 Dual-Fuel engine equipped with HS was tested for full load performance at 1000 ~ 1500 rpm with the maximum and minimum HS hydraulic turbine inlet pressure achieved by the engine driven pump selected. Maximum and minimum hydraulic turbine inlet pressures achieved are plotted against engine speed as shown in Figure 40.

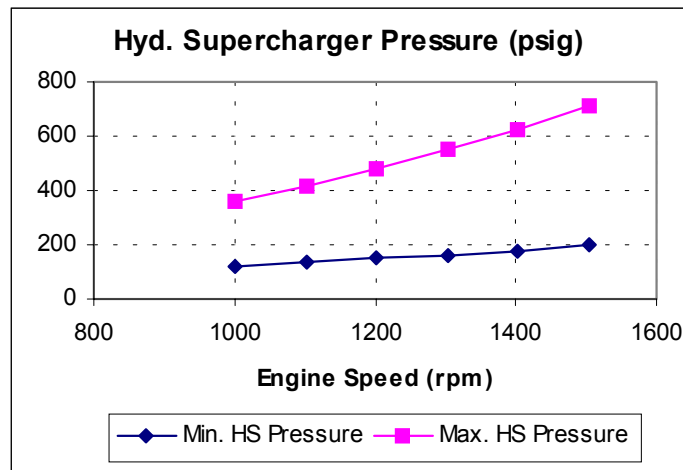


Figure 40: Hydraulic Turbine Inlet Pressure Range

Other engine parameters including emissions were plotted against engine speeds at maximum and minimum hydraulic turbine inlet pressures, as shown in Figures 41 ~ 49 below.

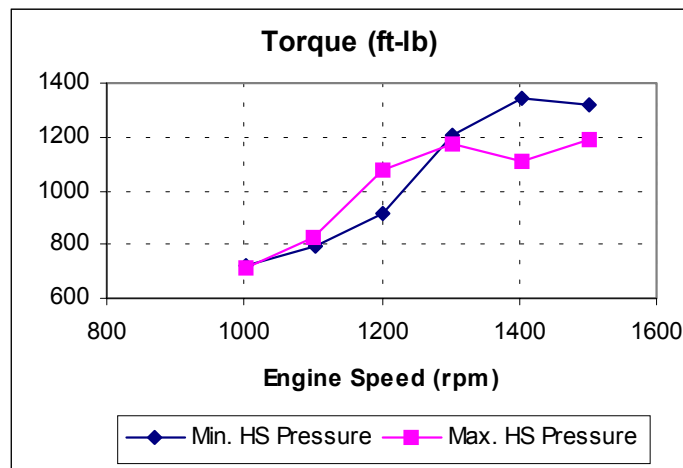


Figure 41: Maximum Torque Achieved

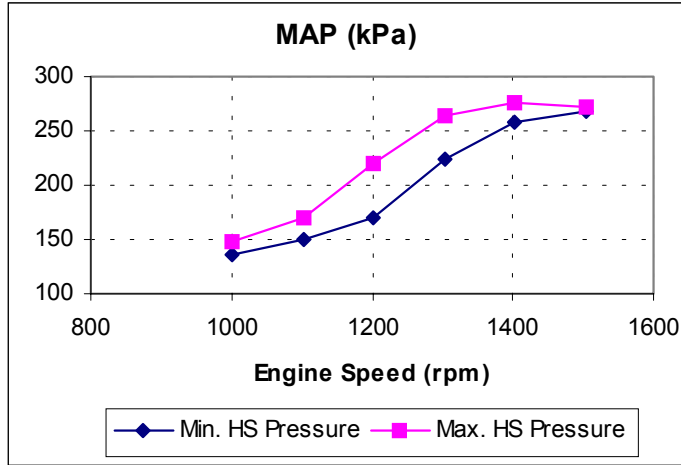


Figure 42: Manifold Absolute Pressure at 100% Load

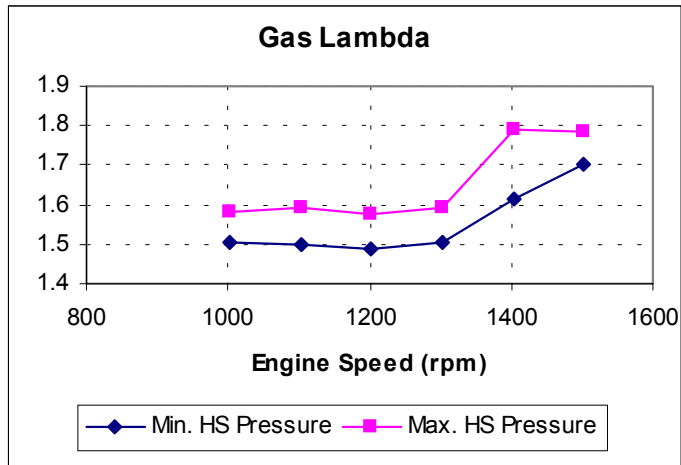


Figure 43: Gas Lambda at 100% Load

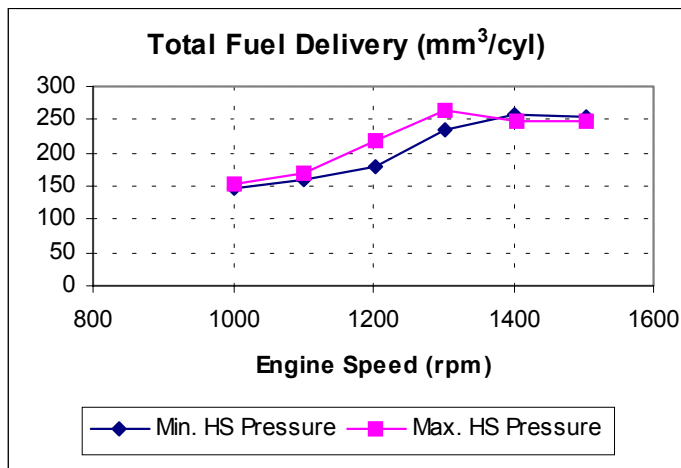


Figure 44: Fuel Delivery at 100% Load

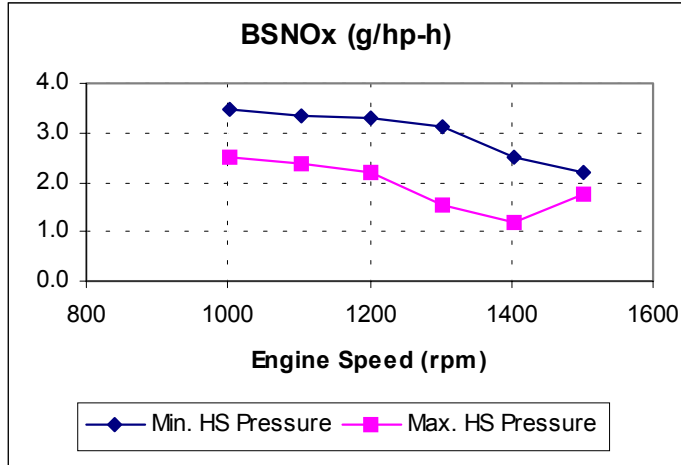


Figure 45: NOx Emissions at 100% Load

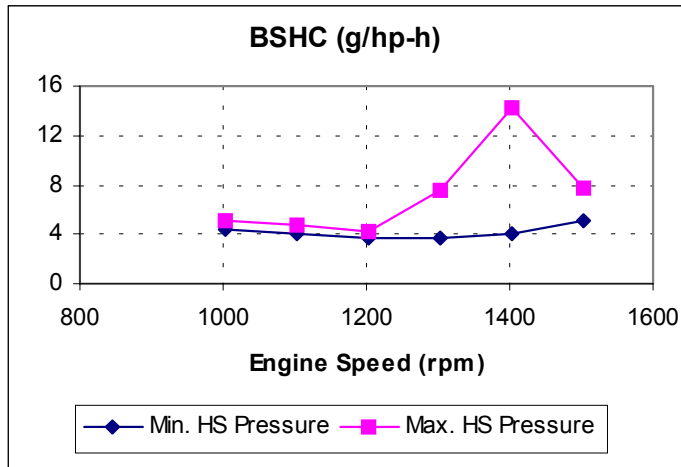


Figure 46: HC Emissions at 100% Load

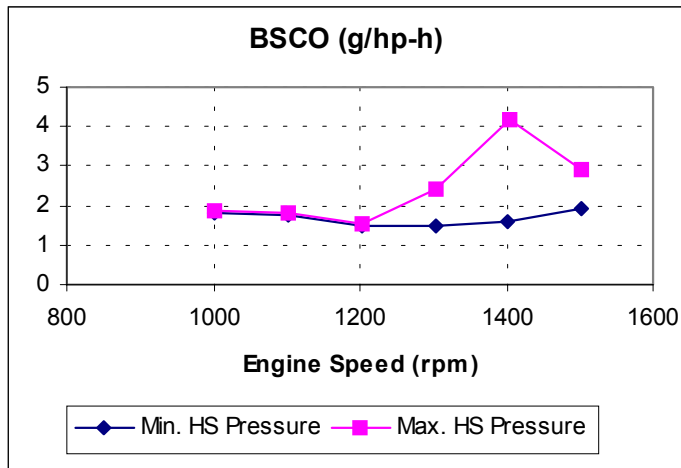


Figure 47: CO Emissions at 100% Load

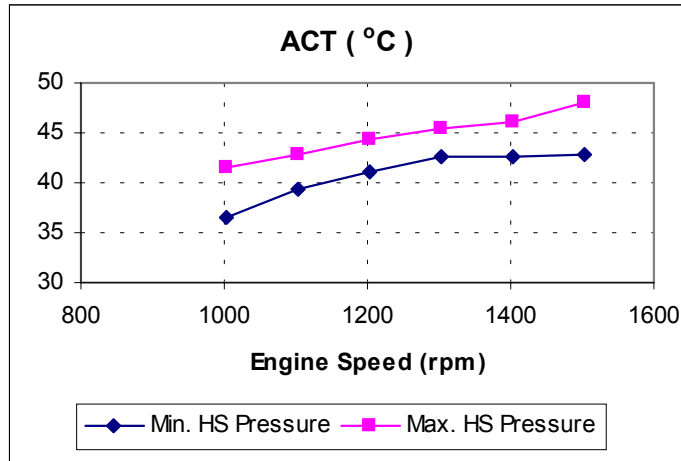


Figure 48: ACT at 100% Load

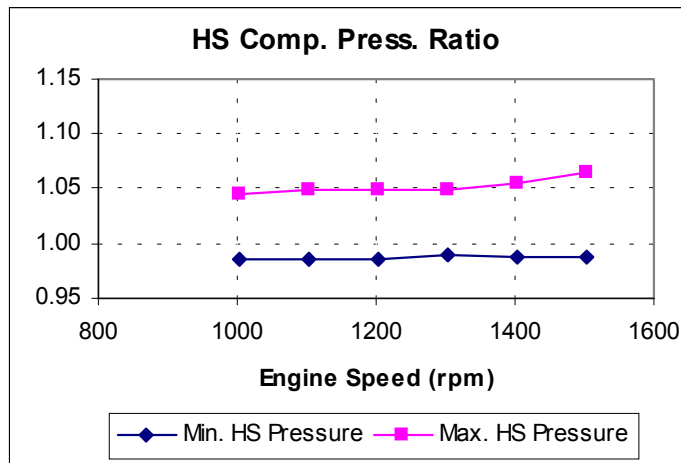


Figure 49: HS Compression Pressure Ratio at 100% Load

The following summarizes test results and findings:

- 1) Maximum torque was plotted against engine speeds as shown in Figure 41. Lower torque was observed at engine speeds above 1300 rpm when HS turbine pressure was set to maximum. This was due to the increased gas lambda as MAP increased as shown in Figures 42 and 43, while actual fuel delivery remained constant as indicated in Figure 44. Desired torque rise characteristics will be achieved by optimization and calibrations of engine parameters.
- 2) It is possible to achieve 1450 lb-ft at 1200 rpm if sufficient air charge is available. Total fuel delivery would be increased to 270 mm³/cyl approximately as long as gas lambda of 1.5 is maintained.
- 3) NO_x, HC and CO emissions were plotted against engine speeds as shown in Figures 45 ~ 47. It is evident that gas lambda is the engine parameter that affects emissions the most.
- 4) Figure 48 shows that ACT increases as HS turbine inlet pressure increases, which is due to higher HS compression pressure ratio.

5) Figure 49 indicates that the HS compressor CPR is around 1.05 at maximum HS turbine pressure. Actual gaseous fuel injected is being limited due to insufficient air charge at engine speeds below 1400 rpm. It shows that optimization of the HS compressor performance characteristics is required.

6.3.2 Hydraulic Pressure Modulation

The C-12 Dual-Fuel engine equipped with HS was tested for full load performance at 1100 ~ 1400 rpm while HS hydraulic turbine inlet pressure was modulated between the maximum and minimum pressures by the HS EPR.

Engine parameters including emissions were plotted against engine speeds at maximum and minimum hydraulic turbine inlet pressures, as shown in Figures 50 ~ 61 below.

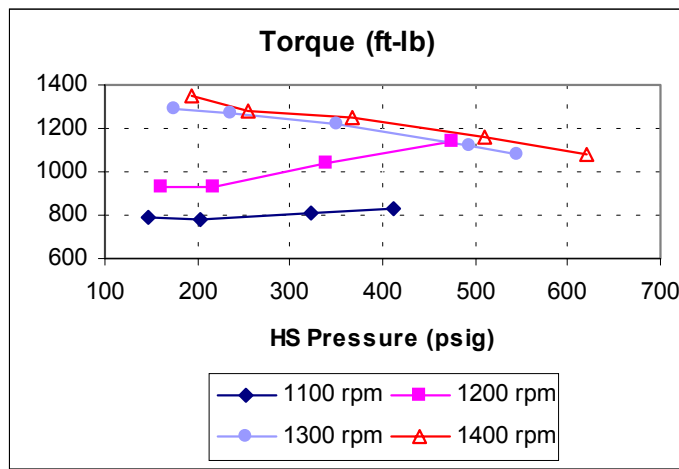


Figure 50: Max. Torque at Various Hyd. Turbine Pressures

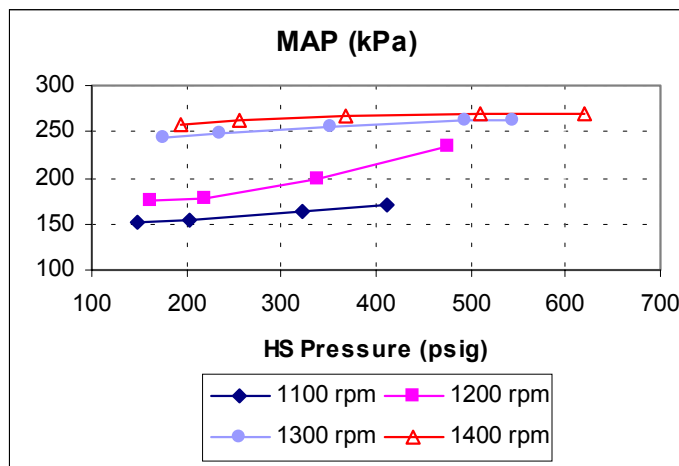


Figure 51: Boost at Various Hyd. Turbine Pressures

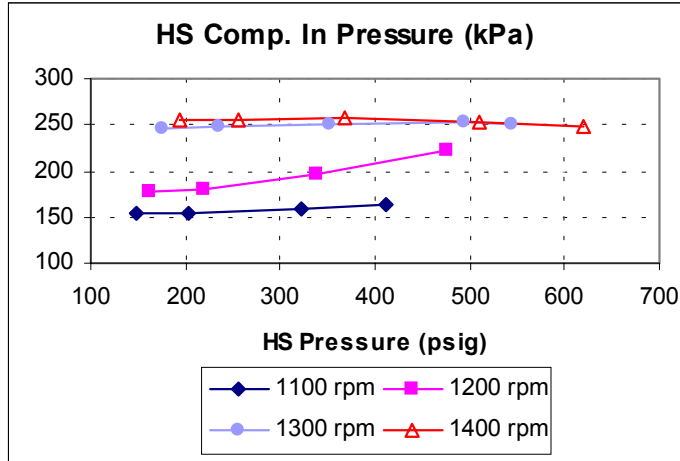


Figure 52: HS Compressor Inlet Pressure at Various Hyd. Turbine Pressures

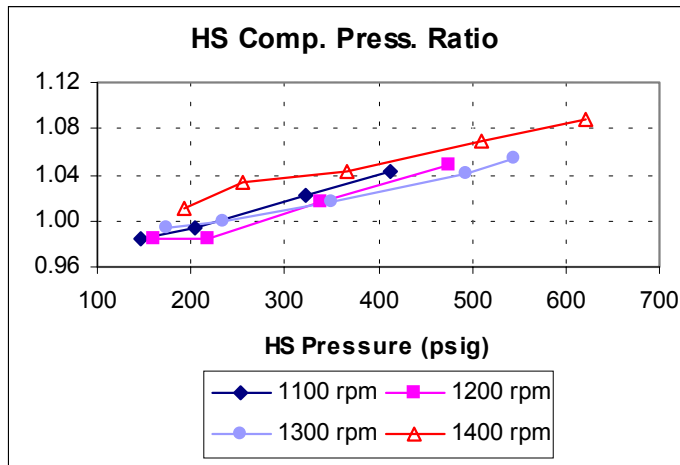


Figure 53: HS Compressor CPR at Various Hyd. Turbine Pressures

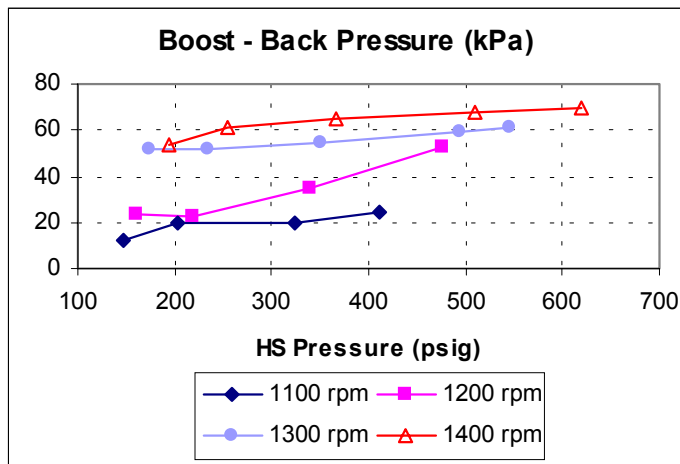


Figure 54: Boost and Back Pressure Difference at Various Hyd. Turbine Pressures

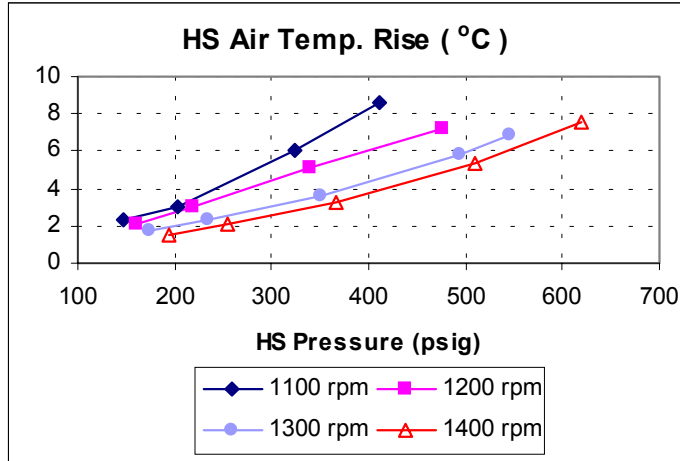


Figure 55: HS Air Temperature Increases at Various Hyd. Turbine Pressures

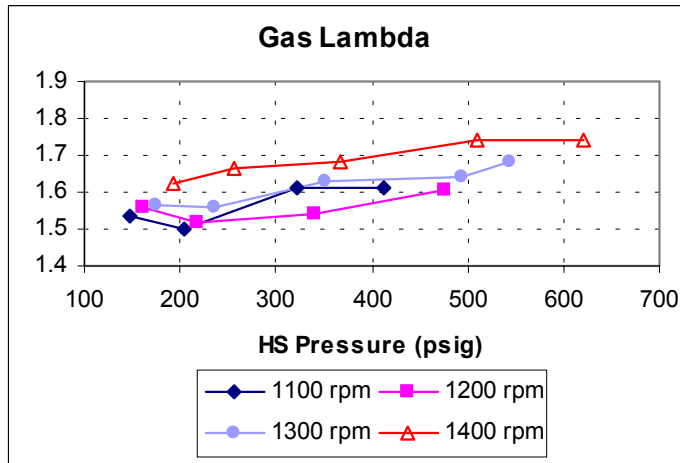


Figure 56: Lambda at Various Hyd. Turbine Pressures

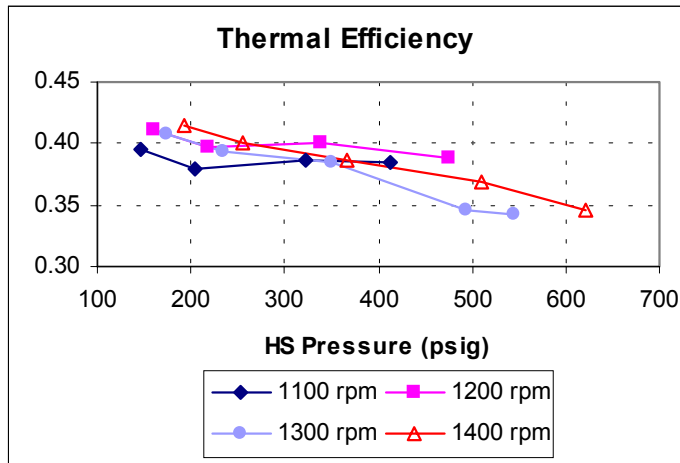


Figure 57: Thermal Efficiency at Various Hyd. Turbine Pressures

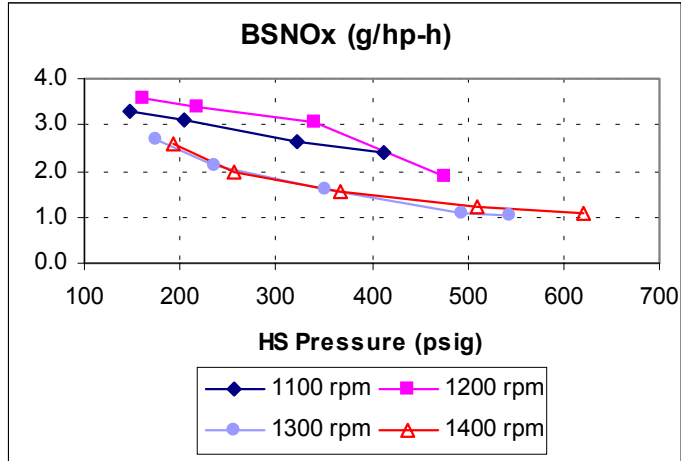


Figure 58: NOx Emissions at Various Hyd. Turbine Pressures

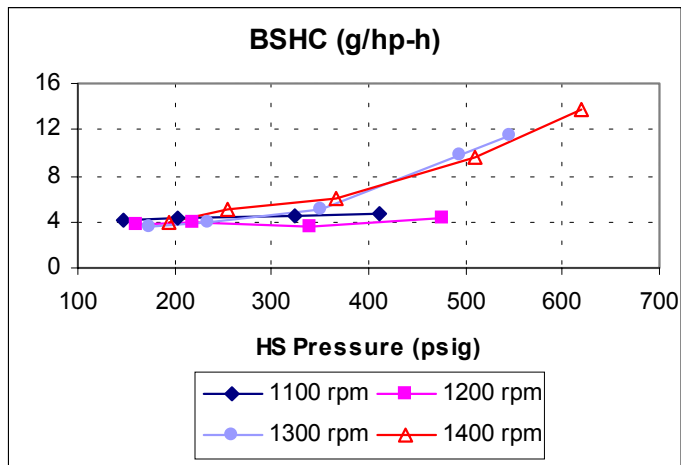


Figure 59: HC Emissions at Various Hyd. Turbine Pressures

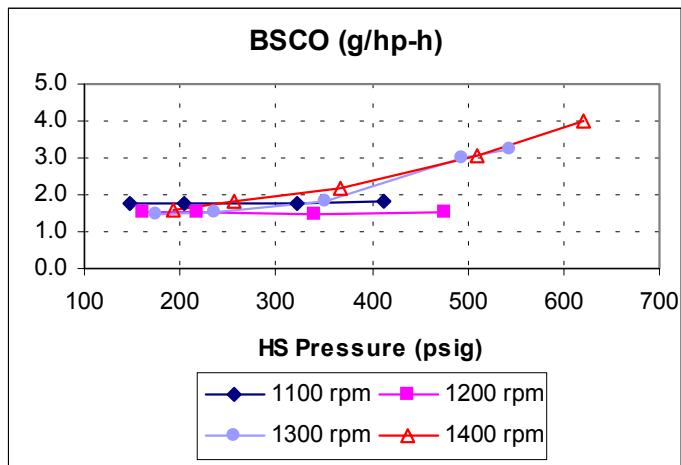


Figure 60: CO Emissions at Various Hyd. Turbine Pressures

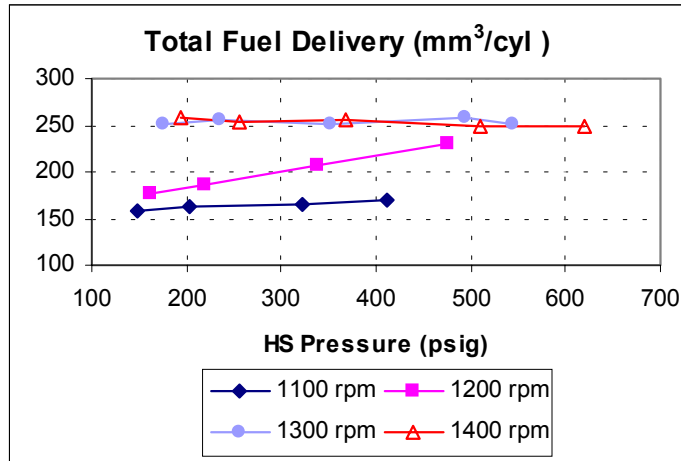


Figure 61: Total Fuel Delivery at Various Hyd. Turbine Pressures

The following summarizes test results and findings on hydraulic pressure modulation:

1. Torque decreases as hydraulic turbine pressure increases at 1300 and 1400 rpm as shown in Figure 50. This is due to the increased lambda resulted from the increased in HS compression pressure ratio, retarded pilot timing and reduced commanded fuel as ACT increases. In addition to the increased lambda, the decreased torque is due to the increased parasitic loss. As HS pressure increases the parasitic loss increases.
2. HS compressor CPR increases as hydraulic turbine pressure increases at constant engine speeds. CPR reached almost 1.1 at 1400 rpm as shown in Figure 53.
3. ACT increases as hydraulic turbine pressure increases. This is due to air temperature rise in the HS compressor as shown in Figure 55.
4. NOx emissions decreases as hydraulic turbine pressure increases as shown in Figure 58. This is due to the leaner air and gas mixture at higher hydraulic turbine pressure. Figure 56 shows gas lambda vs hydraulic turbine pressure at various engine speeds.

6.3.3 Application and Feasibility

The HS definitely has its merits on boosting air mass flow required by the enhanced C-12 Dual-Fuel engine at engine speeds below 1400 rpm. At engine speeds above 1600 rpm, the air mass provided by the original exhaust gas turbocharger, in fact is more than what a C-12 Dual-Fuel engine needs at full load. The HS has also proven to be a suitable and valuable device in identifying the turbocharger performance characteristics required by the enhanced C-12 Dual-Fuel engine. The followings are the principal investigator's concerns on applying the HS on the enhanced C-12 Dual-Fuel engines:

1. Over-boost at engine speeds above 1600 rpm. Figure 33 in Section 6.3.1 shows that MAP exceeds 300 kPa at engine speeds between 1500 ~ 1800 rpm. HS pressure shall be electronically controlled as a function of engine speed and load.
2. Higher TAB valve capability is needed to maintain optimum lambda at engine speeds above 1600 rpm at full load.

3. Hydraulic turbine inlet pressure controls and its resolution is not adequate using the existing HS configuration. Further development and optimization on pump delivery and speed, and/or hydraulic turbine nozzle of the HS system is necessary.
4. The HS compressor CPR is not optimized. CPR of less than 1.05 is not high enough at 1200 rpm engine speed, the peak torque speed of C-12 Dual-Fuel engine.
5. HS hydraulic pressure control and governing strategy has to be developed and tested for transient response. The engine speed governing and TAB valve control have been well matched in the current base C-12 Dual-Fuel engine, optimum lambda is resulted cycle-by-cycle and cylinder-by-cylinder. Engineering effort is required in harmonizing the hydraulic supercharger with existing turbocharger and TAB for optimum lambda.
6. Air charge temperature rise in the HS compressor. Extra air charge after-cooling may be necessary.
7. Parasitic loss of 13 hp is expected at 1600 rpm, minimum HS hydraulic pressure. An electric clutch installed at the hydraulic pump drive may be considered to reduce the parasitic loss further at high engine speeds.

6.4 Other Activity on Air Pressure Booster

There has been a concern on "commercial viability" of the enhanced C-12 Dual-Fuel engine having the combination of technologies incorporated as originally proposed. When the proposal was made to NREL and AQMD, the Kapich hydraulic supercharger was the known available component that would provide a straightforward way to achieve added boost. Turbocharger incorporating a variable nozzle turbine (VNT), intended for heavy-duty highway truck diesel engines in the 12 ~ 14 liters displacement range, was also unknown. The single turbocharger, equipped with a VNT, will be attractive with a minimum change required in installation volume, and closed-loop lambda control from the Dual-Fuel engine ECU is possible.

It is worth evaluating another turbocharger of conventional type, which will provide the added boost at low engine speed. Prior to identifying the best combination meeting the project objectives, re-matching a conventional turbocharger was considered.

A single turbocharger either with or without a VNT will be attractive. Minimum change will be required in installation volume. Closed-loop lambda control currently used on the Dual-Fuel engine will be retained on the enhanced C-12 Dual-Fuel engine. The overall compression pressure ratio which includes the HS is plotted against the engine speed at full load as shown in Figure 62. It is the principal investigator's opinion that another turbocharger of conventional type shall be evaluated. The desired turbocharger shall have compression pressure ratio of 2.6 approximately, at 1200 rpm engine speed, exhaust wastegate shall be actuated at 270 kPa. Engineering efforts on matching a single turbocharger for the enhanced C-12 Dual-Fuel engine will be preferable instead of optimizing an additional hydraulic supercharging system.

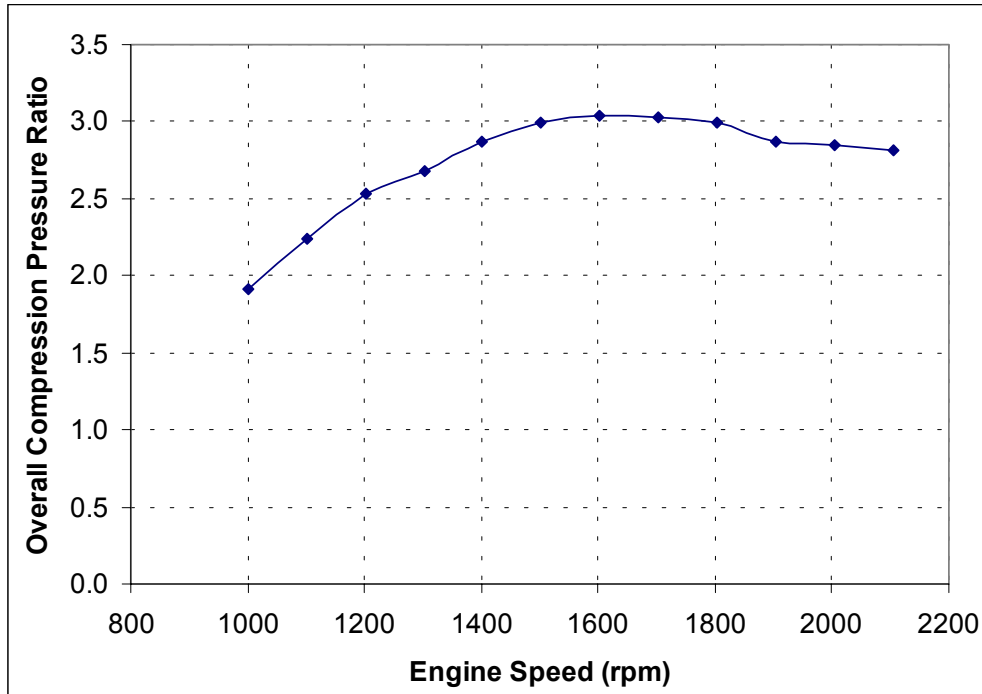


Figure 62: Overall Compression Pressure Ratio at Full Load

6.4.1 Turbocharger with Smaller A/R Turbine

The base C-12 Dual-Fuel engine uses the original turbocharger that comes with the diesel engine. It is a Garrett® GT42 wastegated turbo with a 1.44 A/R turbine housing. A 1.28 A/R non-wastegated turbine housing which is interchangeable was received from Garrett Engine Boosting System. Having a smaller area-to-radius ratio, it is expected that higher boost would be produced.

Engine test was conducted using the turbocharger which had the original turbine housing replaced with the 1.28 A/R non-wastegated turbine housing. Tests were focused on full load at engine speeds from 1100 ~ 1400 rpm, on Dual-Fuel operation as well as 100% diesel for comparison.

Engine parameters including NOx emissions were plotted against engine speeds as shown in Figures 63 ~ 71 below:

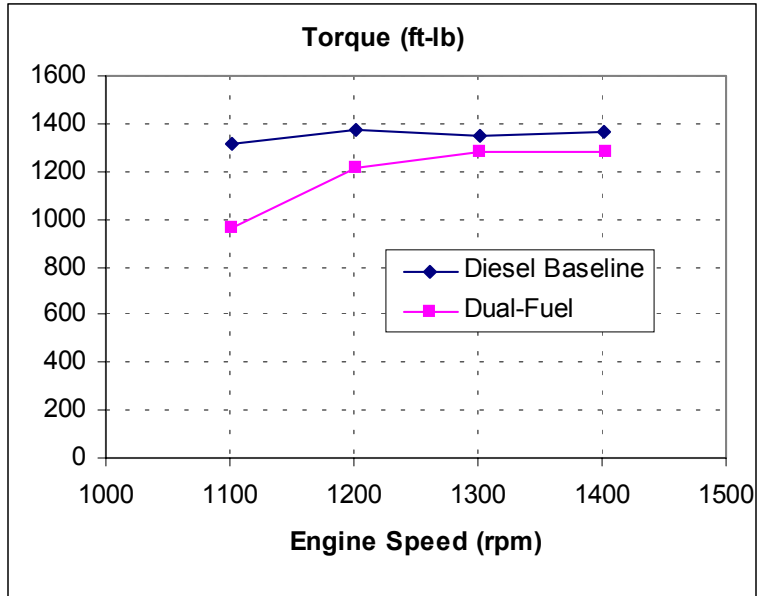


Figure 63: Max. Torque with 1.28 A/R Turbo

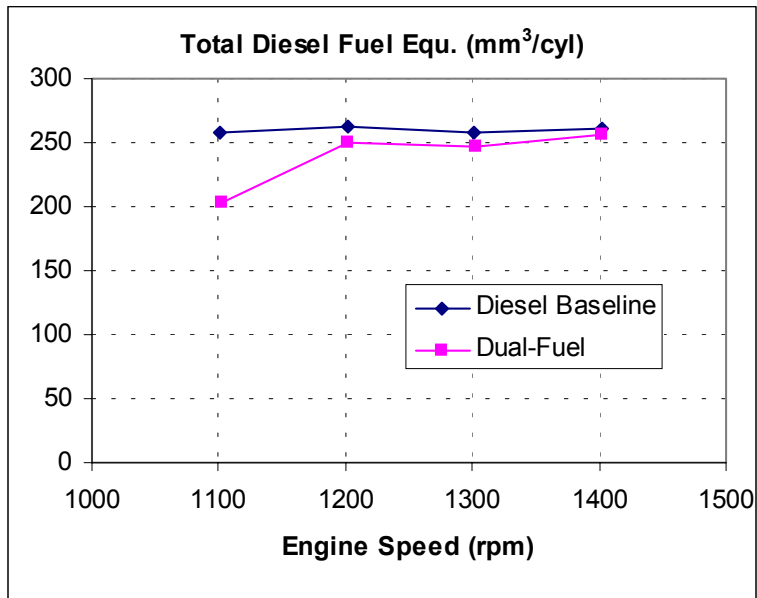


Figure 64: Total Fuel Delivery at Full Load with 1.28 A/R Turbo

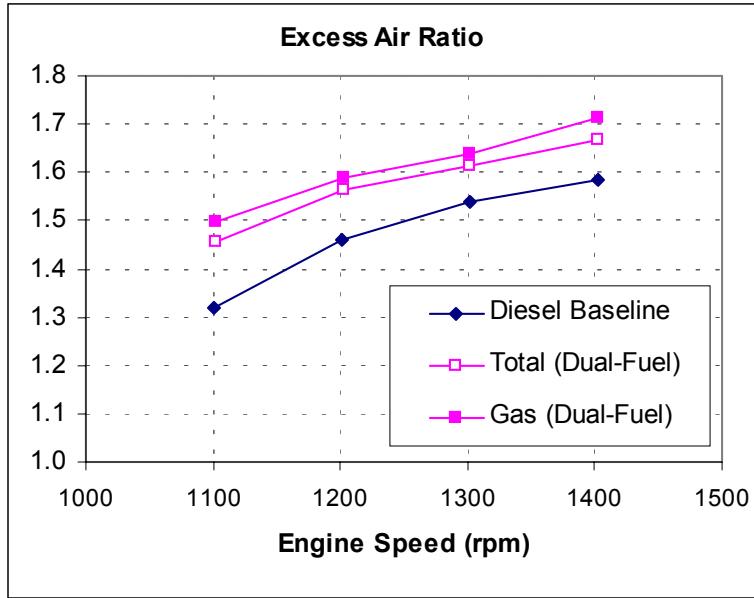


Figure 65: Excess Air Ratio at Full Load with 1.28 A/R Turbo

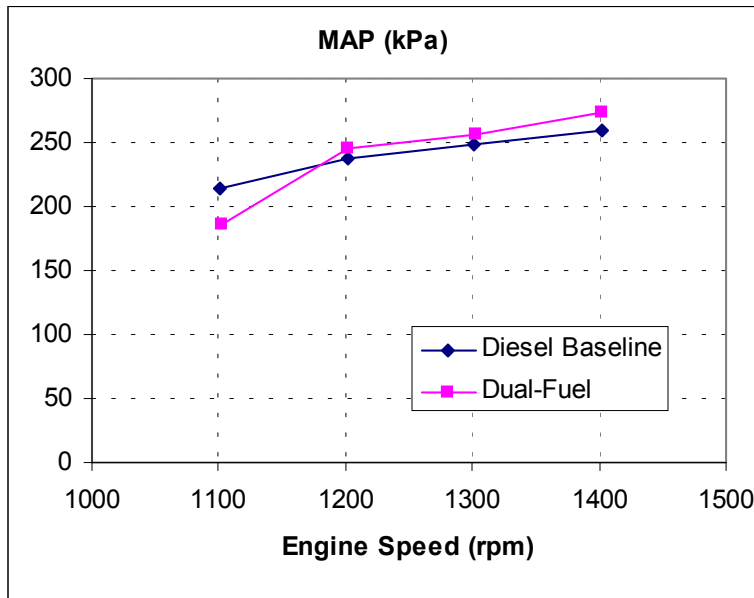


Figure 66: Boost at Full Load with 1.28 A/R Turbo

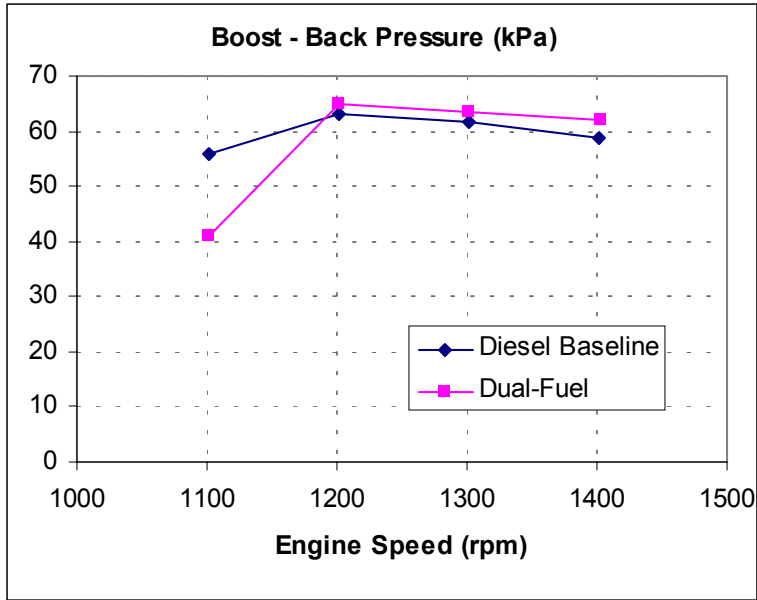


Figure 67: Boost and Back Pressure Difference at Full Load with 1.28 A/R Turbo

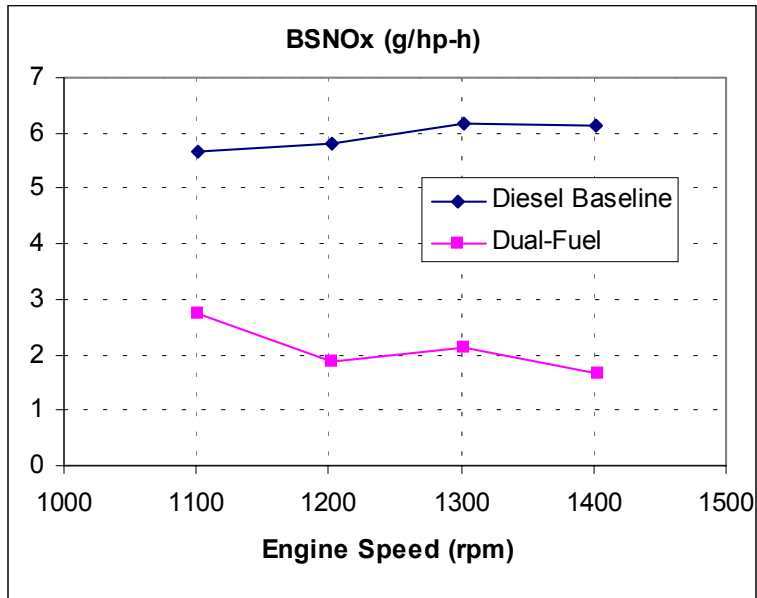


Figure 68: NOx Emissions at Full Load with 1.28 A/R Turbo

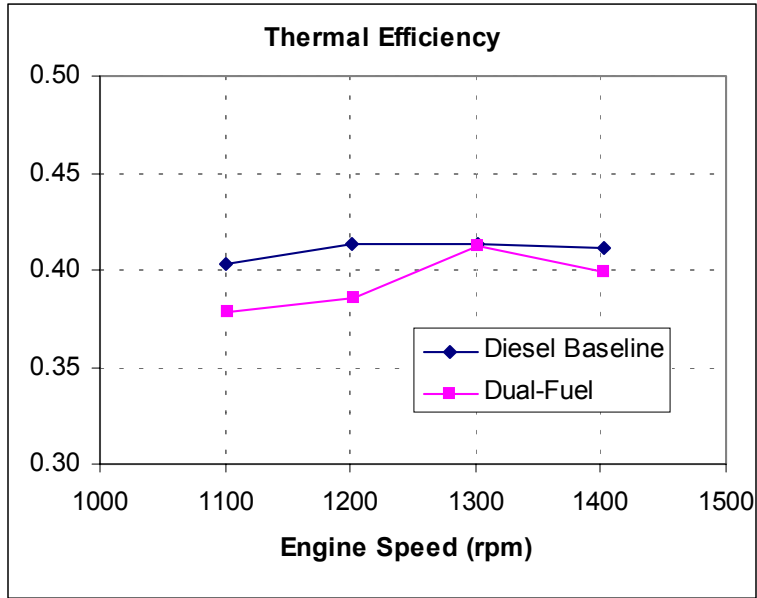


Figure 69: Thermal Efficiency at Full Load with 1.28 A/R Turbo

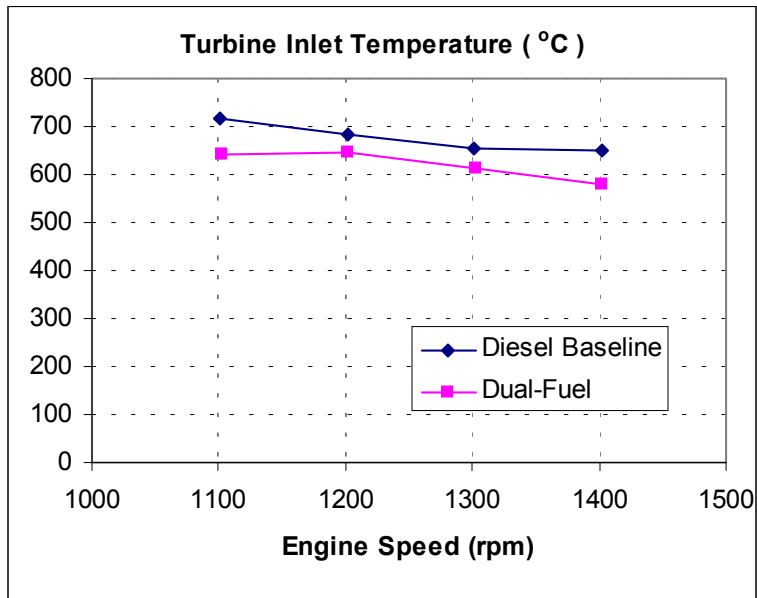


Figure 70: Turbine Inlet Temperature at Full Load with 1.28 A/R Turbo

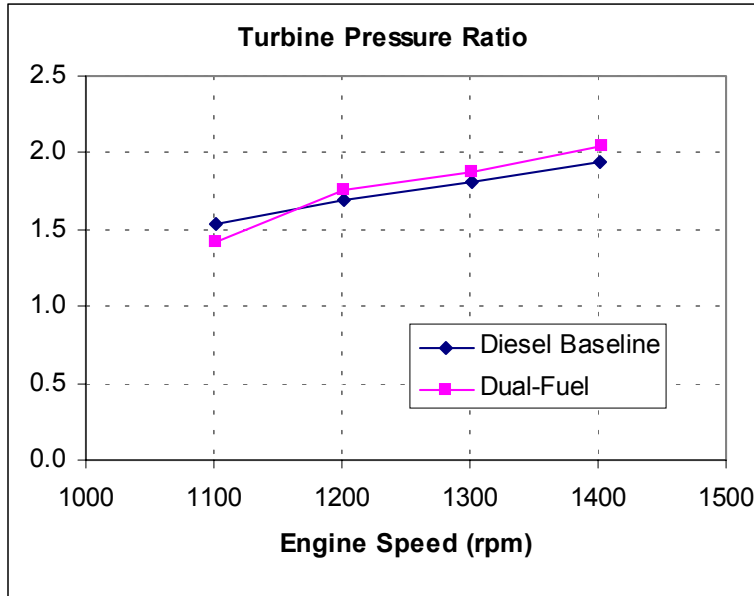


Figure 71: Turbine EPR at Full Load with 1.28 A/R Turbo

The following summarizes test results and findings:

1. Torque peaks at 1280 lb-ft at 1300 rpm.
2. Gas lambda was maintained above the rich limit of 1.50 as shown in Figure 65. Higher torque can be achieved when lambda is maintained at 1.50.
3. Lambda is relatively much lower when running on 100% diesel, comparing to Dual-Fuel operation as shown in Figure 65.
4. NOx emissions was around 2.0 g/hp-h on Dual-Fuel as compared to 6.0 g/hp-h on 100% diesel.
5. Turbine inlet temperature is lower when running on Dual-Fuel as shown in Figure 70. This is due to the higher excess air ratio as shown in Figure 65.
6. Occasional knock occurred when boost pressure exceeded 270 kPa.
7. Lambda rich limit shall be a function of MAP in addition to ACT to avoid engine knock. A leaner air and gas mixture is required as MAP increases.
8. Efficiency decreases as lambda increases beyond its optimal value due to the lower bulk gas temperature and slower flame speed. Incomplete combustion of the fuel and cycle-to-cycle variation increase as the combustible mixture becomes too lean. It is therefore likely that torque output may not increase proportionally with increased fuel delivery when higher boost is available.

7 Summary and Conclusions

The following technologies were investigated during this project under both NREL and AQMD contracts:

1. Knock detection and control
2. Turbo expansion to lower ACT
3. Air pressure booster in addition to the stock turbocharger

Due to the announcement made by Caterpillar on March 6, 2001, that all Cat truck engines including C-12 will employ the new engine technology called ACERT, or

Advanced Combustion Emissions Reduction Technology. The mechanically actuated electronic unit injector (MEUI) fuel system employed currently on the C-12 truck engine will be replaced with the next generation HEUI™ fuel system. Engine design change is required to accommodate the HEUI fuel system. The technologies developed during this project will become inappropriate. Commercialization of these technologies as originally envisioned is therefore not possible. It was determined in the interest of all parties concerned, that BKM and CAP stop work on this project at the end of March 2001.

Nevertheless, the technical investigation and development of the enhanced C-12 Dual-Fuel engine has been conducted. Conclusions drawn from the investigation described in this report are summarized as follows:

1. Caterpillar 142-0215 knock sensor is the best choice of accelerometer type of knock sensors for the enhanced C-12 Dual-Fuel engines. It requires less effort to integrate the sensor's electronic control module to the Dual-Fuel truck engine ECM.
2. One sensor covering two adjacent cylinders has produced reliable results on knock detection, although choice of sensor location is restricted by the availability of tapped holes on engine block currently produced. Caterpillar will be consulted if additional tapped holes
3. Knock detection algorithm were developed and tested. Knock sensor signals were monitored within a programmable crank angle based window for each individual cylinder.
4. Knock control strategies and algorithm were developed, testing of which was not completed.
5. Unlike diesel engine, the lean-burn Dual-Fuel engine has total control of lambda which makes the reduced ACT have no significant effect on performance and emissions.
6. Gas lambda and pilot timing are two dominating factors on performance and emissions for lean-burn Dual-Fuel engine.
7. Hydraulic supercharger has its merits on boosting air mass flow required by the enhanced C-12 Dual-Fuel engine at engine speeds below 1400 rpm. It has also proven to be a valuable device in identifying the turbocharger performance characteristics required by the enhanced C-12 Dual-Fuel engine.
8. There are concerns on commercial viability of the enhanced C-12 Dual-Fuel engine having the hydraulic supercharging system incorporated. A single VNT turbocharger optimized for Dual-Fuel engine is the best solution for the enhanced C-12 Dual-Fuel engine.
9. Higher boost increases the knock tendency. Lambda rich limit shall be a function of MAP and ACT.

**Preliminary turbo expander calculation based on engine data at
1200 rpm, 1450 ft-lb on diesel**

	Symbol	INPUT	OUTPUT	Unit
Efficiency of exhaust turbocharger compressor	η_{c1}	0.70		
Efficiency of turboexpander compressor	η_{c2}	0.70		
Efficiency of exhaust turbocharger turbine	η_{t1}	0.74		
Efficiency of turboexpander turbine	η_{t2}	0.70		
Exhaust turbocharger turbine pressure ratio	EPR_1	1.80		
Turboexpander turbine pressure ratio	EPR_2	1.35		
Exhaust turbocharger compressor pressure ratio	CPR_1	2.55		
Turboexpander compressor pressure ratio	CPR_2	1.50		
Turboexpander aftercooler flow coefficient	P_3/P_2	0.95		
Exhaust turbocharger aftercooler flow coefficient	P_5/P_4	0.95		
Effectiveness of turboexpander aftercooler	$(T_4-T_5)/(T_4-T_3)$	1.20		
Effectiveness of exhaust turbocharger aftercooler	$(T_2-T_3)/(T_2-T_1)$	0.93		
Turboexpander aftercooler temperature drop	$T_4 - T_5$		64.32	°C
Exhaust turbocharger aftercooler temp. drop	$T_2 - T_3$		120.50	°C
Air mass flow		18.25		kg/min
Exhaust turbocharger compressor inlet temperature	T_1	24.00		°C
Exhaust turbocharger compressor outlet temperature	T_2		153.57	°C
Turboexpander compressor inlet temperature	T_3		33.07	°C
Turboexpander compressor outlet temperature	T_4		86.67	°C
Turboexpander turbine inlet temperature	T_5		22.35	°C
Turboexpander turbine outlet temperature	T_6		5.36	°C
Exhaust turbocharger turbine inlet temperature	T_8	689.00		°C
Exhaust turbocharger turbine outlet temperature	T_9		589.57	°C
Exhaust turbocharger compressor inlet pressure	P_1	100.00		kPa
Exhaust turbocharger compressor outlet pressure	P_2		255.00	kPa
Turboexpander compressor inlet pressure	P_3		242.25	kPa
Turboexpander compressor outlet pressure	P_4		363.38	kPa
Turboexpander turbine inlet pressure	P_5		345.21	kPa
Turboexpander turbine outlet pressure	P_6		255.71	kPa
Exhaust turbocharger turbine inlet pressure	P_8	187.00		kPa
Exhaust turbocharger turbine outlet pressure	P_9		103.89	kPa

Calculations				
Constant c_p between state 1 and state 2	C_{p1-2}	1.008		kJ/kg-K
Constant k between state 1 and state 2	k_{1-2}	1.398		
	T_{2s}		387.70	K
Constant c_p between state 3 and state 4	C_{p3-4}	1.006		kJ/kg-K
Constant k between state 3 and state 4	k_{3-4}	1.399		
	T_{4s}		343.59	K
Constant c_p between state 5 and state 6	C_{p5-6}	1.004		kJ/kg-K
Constant k between state 5 and state 6	k_{5-6}	1.400		
	T_{6s}		271.08	K
Constant c_p between state 8 and state 9	C_{p8-9}	1.121		
Constant k between state 8 and state 9	k_{8-9}	1.344		
	T_{9s}		827.63	K